APPLICABILITY OF HEAT MIRRORS IN REDUCING THERMAL LOSSES IN CONCENTRATING SOLAR COLLECTORS

A Dissertation submitted

in the partial fulfilment of the requirements

for the award of degree of

Master of Engineering (M.E.)

in

Thermal Engineering

by

PRASHANT MAHENDRA

Registration No.: 801483018

Under the supervision of

Dr. MADHUP KUMAR MITTAL

(Assistant Professor)

Dr. VIKRANT KHULLAR

(Assistant Professor)

DEPARTMENT OF MECHANICAL ENGINEERING

THAPAR UNIVERSITY, PATIALA-147004, INDIA

June 2016

CERTIFICATE

I, Prashant Mahendra, declare that the dissertation entitled **"Applicability of heat mirrors in reducing thermal losses in concentrating solar collectors",** is an authentic record of my work carried out as requirements for the award of the degree of **Master of Engineering** in **Thermal Engineering** at **Thapar University, Patiala** under the supervision of **Dr. Madhup K. Mittal,** Assistant professor, Mechanical Engineering Department, **and Dr. Vikrant Khullar,** Assistant professor, Mechanical Engineering Department, Thapar University, Patiala during July 2014 to June 2016. No part of the matter embodied in this report has been submitted to any other university or institute for the award of any degree.

Date: 14-7-2016
Place: Patiala

Prashant Mahendra
Roll No.801483018
Thapar University, Patiala

This is to certify that above statement made by the candidate is correct and true to the best of my knowledge.

Dr. Madhup K. Mittal
Assistant Professor
Mechanical Engineering Department
Thapar University, Patiala

Dr. Vikrant Khullar
Assistant Professor
Mechanical Engineering Department
Thapar University, Patiala

Countersigned by

Dr. S. K. Mohapatra
Sr. Professor and Head
Mechanical Engineering Department
Thapar University, Patiala

Dr. S. S. Bhatia
Dean, Academic Affair
Thapar University, Patiala

ACKNOWLEDGMENTS

I am very thankful to my supervisors. I am sincerely glad that I got the supervisors like ***Dr. Madhup K. Mittal*** and ***Dr. Vikrant Khullar***. Both of them really boost me to go in the right direction for my research work as well as for the life coming in future. The love, care, affection, patience, which they showed, I really appreciate that. Every time when I made mistake, they guide me like I am a kid, I am very thankful to them for being so kind. I really appreciate the exposer, the opportunity, and the environment provided by the Thapar University, Patiala, to carry out the research work are highly appreciated.

A special thanks to ***Dr. Vikrant Khullar*** for being there for me, whenever I needed him. You treated me more like your younger brother and gave your priceless advice, which I will never forget, I really appreciate your kindness, and I am very sorry for the mistakes which I did, but you always ignored them.

Last but not the least, I am forever grateful to My Parents and family especially ***MY FATHER,*** he always boosted me to follow my heart and live my own life. I am very thankful to friends, for their unforgettable support and best wishes, I want to thank to all the people who are in my life to guide and teach me to step further and forget the rest, THANK YOU.

(Prashant Mahendra)

Dedicated to

My loving FAMILY

ABSTRACT

Flux distribution around the parabolic trough receiver being typically non-uniform, only a certain portion of the receiver circumference receives the concentrated solar irradiance. However, radiative and convective losses occur across the entire receiver circumference. The present work attempts to introduce the idea employing transparent heat mirror to effectively reduce the heat loss area and thus improve the thermal efficiency of the solar collector. Transparent heat mirror essentially has high transmissivity in the solar irradiance wavelength band and high reflectivity in the mid-infrared region thus it allows the solar irradiance to pass through but reflects the infrared radiation back to the solar selective metal tube. Practically, this could be realized if certain portion of the conventional low iron glass envelope is coated with Sn-In_2O_3 so that its acts as a heat mirror. The spatial flux distribution around the receiver dictates the region of the glass envelope which needs to be coated with Sn-In_2O_3 so that thermal losses could be significantly reduced without hampering the optical efficiency of the collector.

In the present study, a parabolic receiver design employing the aforesaid concept has been proposed. Detailed heat transfer model has been formulated. The theoretical modelling results have been compared to the results pertinent to a corresponding conventional concentrating parabolic solar collectors in the literature. It was observed that under similar operating conditions the heat mirror-based parabolic trough concentrating solar collector has about 3-12% higher thermal efficiency as relative to the conventional parabolic trough design. Furthermore, steady state heat transfer analysis reveals that depending on the solar flux distribution there is an optimum circumferential angle ($\theta = \theta_{optimum}$), where θ is the heat mirror circumferential angle) up to which the glass envelope should be coated with Sn-In_2O_3. For angles higher than the optimum angle, the collector efficiency tends to decrease owing to increase in optical losses. Finally, the analysis revealed that the magnitude of efficiency enhancement is pronounced at high receiver temperatures. Thus as a whole, the proposed receiver design promises higher thermal efficiencies and lower thermal losses as compared to the conventional parabolic trough receiver designs particularly at high receiver temperatures.

Keywords: Solar energy, parabolic trough collector, non-uniform heat flux, heat mirror.

TABLE OF CONTENTS

LIST OF FIGURES

LIST OF TABLES

NOMENCLATURE

A_1	Inner cross-section area of the receiver tube [m^2]
A_{ap}	Aperture area [m^2]
A_{s1}	Inner surface area of the receiver tube [m^2]
A_{s2}	Outer surface area of the receiver tube [m^2]
A_{s3}	Inner surface area of the glass tube [m^2]
A_{s4}	Outer surface area of the glass tube [m^2]
C, m, n	Constants
$C_0 - C_4$	Model coefficient [Zemler, M. K. et al., 2013]
C_{pf}	Specific heat of heat transfer fluid [$Jkg^{-1}K^{-1}$]
C_{pg}	Specific heat of glass [$Jkg^{-1}K^{-1}$]
D_1	Inner diameter of metal receiver tube [m]
D_2	Outer diameter of metal receiver tube [m]
D_3	Inner diameter of glass envelope tube [m]
D_4	Outer diameter of glass envelope tube [m]
F'	Collector efficiency factor
F''	Collector flow factor
F_r	Collector heat removal factor
f_2	Absorber tube's friction factor for inner surface
fl	Focal length [m]

g_1 Average concentrated heat flux for 1st region ($330^o < \theta < 360^o$) [Wm^{-2}]

g_2 Average concentrated heat flux for 2nd region ($260^o < \theta < 330^o$) [Wm^{-2}]

g_3 Average concentrated heat flux for 3rd region ($180^o < \theta < 260^o$) [Wm^{-2}]

h_a Convective heat transfer coefficient between glass envelope and surrounding [$Wm^{-2}K^{-1}$]

h_f Convective heat transfer coefficient for fluid flowing in the receiver tube [$Wm^{-2}K^{-1}$]

h_r Linearized radiation coefficient [$Wm^{-2}K^{-1}$]

k_a Thermal conductivity of air [$Wm^{-1}K^{-1}$]

k_c Thermal conductivity of glass envelope tube [$Wm^{-1}K^{-1}$]

k_{eff} Effective thermal conductivity of air [$Wm^{-1}K^{-1}$]

k_f Thermal conductivity of heat transfer fluid (HTF) [$Wm^{-1}K^{-1}$]

k_r Thermal conductivity of metal receiver tube ($Wm^{-1}K^{-1}$)

L Length of aperture [m]

m_f Mass flow rate of the HTF [kgs^{-1}]

Nu_a Nusselt number for air

Nu_f Nusselt number for HTF

Pr Prandtl number evaluated at $T_{\text{avg}} = \frac{T_a + T_4}{2}$

Pr_1 Prandtl number for HTF evaluated at T_f

Pr_2 Prandtl number of air evaluated at T_r

Pr_4 Prandtl number of air evaluated at T_4

Pr_a	Prandtl number of air evaluated at T_a
$\dot{Q}_{\text{loss}}$	Thermal losses [W]
$\dot{Q}_{\text{loss1}}$	Heat transfer from receiver outer surface to glass inner surface [W]
$\dot{Q}_{\text{loss2}}$	Conduction heat transfer in glass envelope [W]
$\dot{Q}_{\text{loss3}}$	Heat transfer from glass outer surface to atmosphere [W]
$\dot{Q}_{\text{usefull}}$	Rate of sensible heat gain by the HTF [W]
Re_a	Reynold number of air flow over the glass envelope
Re_f	Reynold number of HTF flow in the absorber tube
S	Solar irradiation [Wm^{-2}]
T_a	Air temperature [K]
T_{ci}	Glass inner surface temperature [K]
T_{co}	Glass outer surface temperature [K]
T_f	HTF mean temperature [K]
T_{inf}	HTF inlet temperature [K]
T_r	Receiver temperature [K]
T_{sky}	Sky temperature [K]
t_g	Thickness of envelope tube [m]
t_r	Thickness of receiver tube [m]
U_L	Overall heat loss coefficient [$Wm^{-2}K^{-1}$]
v	Wind speed across the glass envelope [ms^{-1}]

v_f Mass flow rate of the HTF [ms^{-1}]

W Width of aperture [m]

z Concentrated heat flux on the receiver tube [Wm^{-2}]

$\bar{z}$ Effective concentrated heat flux on the receiver tube [Wm^{-2}]

z_{loss} Total optical and thermal loss [Wm^{-2}]

GREEK SYMBOLS

α_m Absorptivity of selectively coated metal receiver tube in the solar irradiation wavelength band

ε_g Emissivity of glass envelop tube

ε_r Emissivity of selective coated metal receiver tube in infrared radiation region

$\eta_{optical}$ Optical efficiency of the parabolic trough collector

$\eta_{thermal}$ Thermal efficiency of the parabolic trough collector

θ Heat mirror angle [°]

$\theta_{optimum}$ Optimum value of the heat mirror angle [°]

μ_a Kinematic viscosity of air [$kgm^{-1}s^{-1}$]

μ_f Kinematic viscosity of HTF [$kgm^{-1}s^{-1}$]

ρ Reflectivity of the aperture trough

ρ_a Density of air [kgm^{-3}]

ρ_f Density of heat transfer fluid [kgm^{-3}]

ρ_g Density of glass envelope [kgm^{-3}]

ρ_l Reflectivity of the parabolic trough concentrator

σ	Stephen-Boltzmann constant ($5.67 * 10^{-8}$) [WmK^{-4}]
τ_g	Transmissivity of the glass envelop (uncoated portion)
τ_h	Transmissivity of the glass envelop (coated portion)
ψ	Rim angle [°]
ΔT	Rise in temperature of the HTF [K]

ABBREVIATIONS

CSP	Concentrating solar power
CTD	Circumferential temperature difference
DNI	Direct normal irradiation
EFS	Efficiency factor for selectivity
GCR	Geometric concentration ratio
HFD	Heat flux distribution
HTF	Heat transfer fluid
MCRT	Monte-Carlo ray trace method
PTC	Parabolic trough collector
SRT	Solar ray trace method

CHAPTER 1

Introduction

1.1 Introduction

This chapter firstly discusses, the basic motivation behind the present work. Subsequently, the existing solar thermal system have been discussed. Finally, a basic introduction about the fundamental basic of the present work has been presented.

1.2 Motivation

With increase in population, the need for energy is escalating. Modern lifestyle uses for comforts have increased the per capita energy consumption to a level which is unsustainable. Furthermore, limited fossil fuel reservoirs the irreversible damage being caused by burning of the fossil fuels have paved the ways for utilization of renewable sources of energy in a more realistic and practical manner. Amongst the various renewable energy resources, solar energy has profound potential. Sun is the biggest source of energy. The solar energy is available throughout the year, free and the most important it is environmental friendly. In countries like India, where poor quality of coal is used as fuel in the thermal power plant. Solar energy could be a major source of energy, for fulfilling our ever growing energy needs. Therefor it is utmost urgent to improve the existing solar energy harnessing system. The present work is one such step in this direction.

1.3 Solar energy harnessing systems

According to the way of harnessing the solar energy, it can be classified in a number of types, but they can be broadly taken in two types.

1. Non-concentrating collectors
2. Concentrating collectors

They can be further classified as tracking system or non-tracking system. Non-tracking system are mainly the non-concentrating type solar collectors. For higher temperature gain, the systems used, are double axis tracking type, such as in solar power tower.

Non-concentrating solar collector systems (such as flat plate collectors or evacuated tube collectors) are effectively used for low temperature applications such as for water or air heating applications. However, in order to have high temperature solar thermal systems, there is a need

to couple the primary solar thermal cycle involving conversion of solar irradiance into the thermal energy of the working fluid to secondary cycles power/refrigeration cycles. Output from primary solar thermal cycle forms the input to these secondary cycles. Now, in order to ensure efficient operation of these secondary cycles and consequently higher overall efficiencies of the whole system, heat transfer fluid (HTF) at sufficiently high temperatures is desired. This motivates the design of solar thermal systems which are capable of capturing high magnitude of incident solar irradiance without increasing the effective thermal loss receiver area, which in turn could lead to high thermal losses since thermal losses are proportional to surface area. Both of these objectives can be achieved by interposing some concentrating optics either reflectors or refractors in between the incident solar irradiance and the receiver. For instance, in the case of linear parabolic troughs, solar irradiance is firstly incident normally on the aperture of the parabolic mirrors and then gets reflected on the linear cylindrical receiver placed at the focal line of the parabolic trough. Consequently, the flux on the receiver has increased by a factor equal to the solar concentration ratio. Which is defined as the ratio of aperture area to the receiver area $\left[C_{ratio} = A_{ap} \middle/ A_{s2} \right]$, without any corresponding increase in the effective heat loss surface area. The maximum theoretical achievable (limited by second law of thermodynamics) solar concentration ratio in the case of point and line type concentrators is 45000 and 212 respectively (Duffie and Beckman, 1993).

1.4 Present solar technologies

1. Flat plate collector
2. Evacuated glass tube collector
3. Parabolic dish collector
4. Power tower system
5. Linear Fresnel reflector system
6. Parabolic trough collector

1.4.1 Flat plate collectors

Flat plate collector is a non-concentrating type of the solar collector system, in this an array of tubes are used with some selective coating of the special optical properties, and the tube is sealed in the glass to minimise the thermal losses. It uses both the direct and diffused solar irradiation. It is used for the low temperature application like air or water heating for domestic purpose (Refer Fig. 1.1).

1.4.2 Evacuated glass tube collectors

Evacuated glass tube is also a non-concentrating type of the solar collector, there is a metal tube enveloped in the glass tube, in the annulus there is vacuum. The metal tube is closed from both sides. In the metal tube, a special fluid is filled, which gets vaporised at the limited temperature range, and when the fluid is vaporised, it comes on top and the latent heat of vaporisation is carried out by water from there in the form of sensible heat. Hence the rise in the temperature of the water takes place (Refer Fig. 1.2).

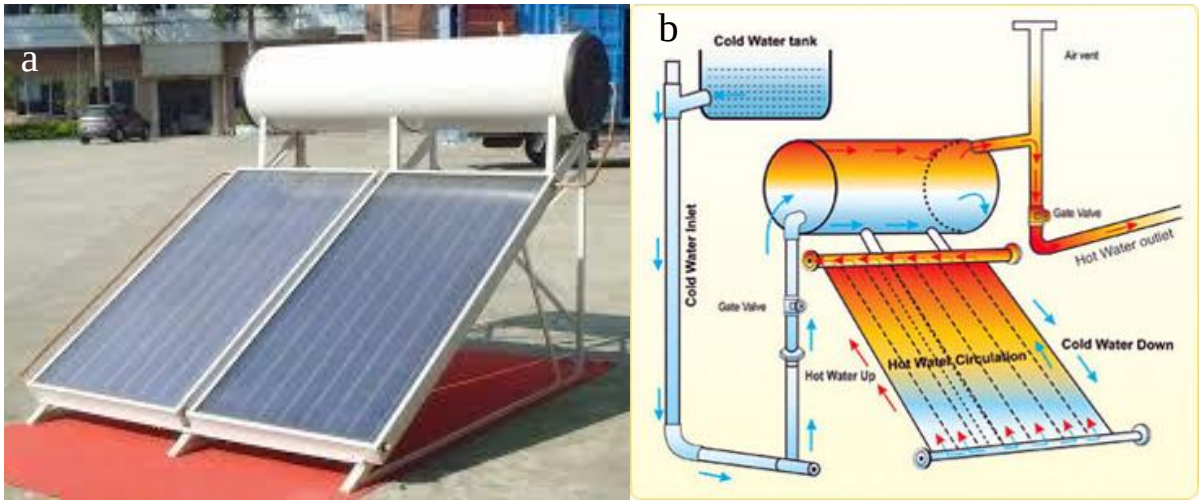

Fig. 1.1 Flat plate collector, (a) Photograph[1], and (b) Schematic diagram[2]

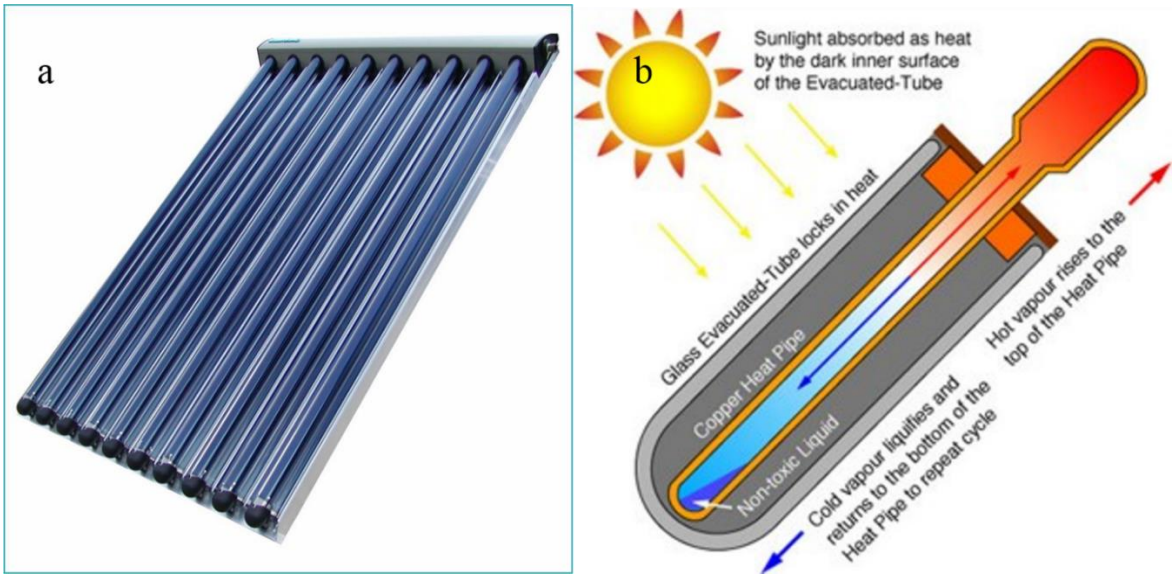

Fig. 1.2 Evacuated glass tube, (a) Photograph[3], and (b) Schematic diagram[4]

[1] http://www.innosolar.cn/UploadFiles/2012323165437102.jpg,
[2] http://chennaiaquatech.com/images/sudarshan-saur/fpc-1.png
[3] http://www.centrometal.hr/wp-content/uploads/2011/12/cvskc-vakumski.jpg
[4] http://hightemp.co.za/evacuated-tube_cross_section.jpg

1.4.3 Parabolic dish collectors

Parabolic dish collector works on the principle of concentrating the solar irradiation to a point. There is a dish type reflector, and the solar irradiation is allowed to fall on the dish reflector, which concentrate all the irradiation onto a point and through this point the HTF is allowed to pass, and the temperature gain is achieved (Refer Fig. 1.3).

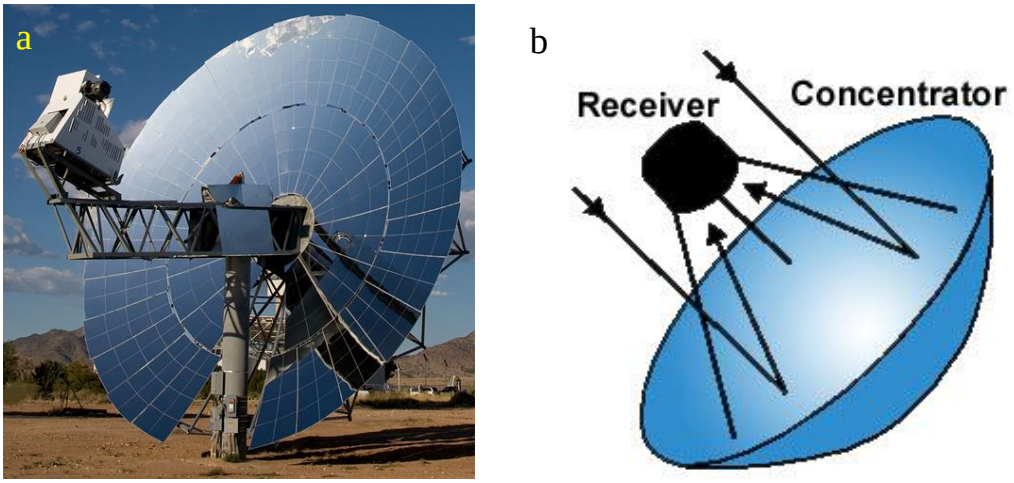

Fig. 1.3 Parabolic dish collector system, (a) Photograph[5], and (b) Schematic diagram[6]

1.4.4 Power tower collector system

Power tower system is also based on the point focusing phenomenon. A power tower has a large tower, which is surrounded by the tracking mirror, also known as the heliostats. A huge area is covered with these heliostats to reflect back all the irradiation on the single point, all the heliostats arrange themselves to track the solar irradiation and to reflect back on the tower. From the tower top, the heat is transferred to the power station by the HTF to produce power (See Fig. 1.4).

1.4.5 Linear Fresnel reflector collector system

Linear Fresnel reflector system is a line focusing system, in this long strips of the mirror are placed in an array, which concentrate the solar irradiation on the fixed linear receiver mounted at some height. It is more likely to function as the parabolic trough system but instead of having the parabolic reflector, it have the array of the linear mirrors. All the mirrors arrange themselves to reflect back the solar irradiation on the long receiver, which is placed at some height. Through that long receiver, the HTF is passed and the rise in temperature is achieved (Refer Fig. 1.5).

[5]http://simms10.wikis.birmingham.k12.mi.us/file/view/suncatcher_medium_photo.jpg/221706524/suncatcher_medium_photo.jpg
[6]http://www.pres.org.pk/wp-content/uploads/2011/08/image0071.jpg

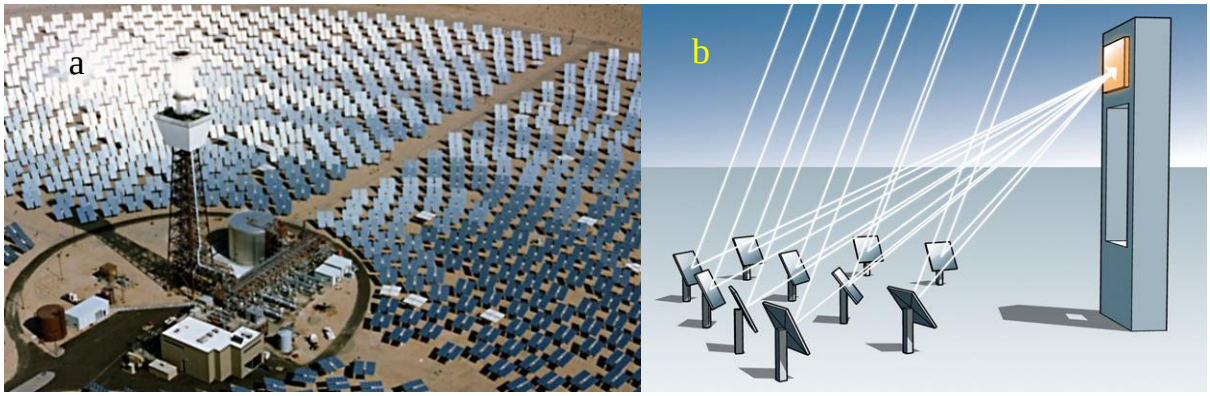

Fig. 1.4 Power tower, (a) Photograph[7], and (b) Schematic diagram[8]

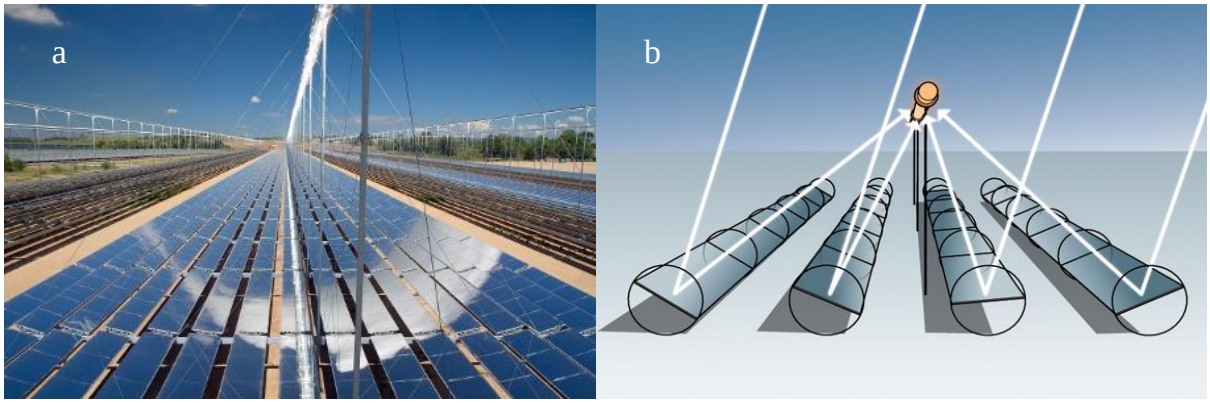

Fig. 1.5 Fresnel linear collector, (a) Photograph[9], and (b) Schematic diagram[10]

1.4.6 Parabolic trough collector

In a parabolic trough all the normal incident solar irradiation on the aperture is concentrated to focus on a line. A receiver tube is placed at the focal line, and through this tube the heat transfer fluid (HTF) is allowed to pass. The solar energy is converted into the thermal energy by the heat transfer mechanism (Refer Fig 1.6).

Since the parabolic trough collector technology is the most mature technology ([11]) among all the solar technologies, so our main focus will be on the parabolic trough technology.

[7] http://planetsave.com/wp-content/uploads/2015/05/concentrated-solar-power-screenshot-from-eia.gov_.jpg
[8] http://www.energy.siemens.com/ru/pool/hq/power-generation/power-plants/csp/solar_tower_large.jpg
[9] https://williampaulbell.files.wordpress.com/2014/11/120628_novatec_solar_solar_boiler_liddell_1.jpg
[10] http://www.energy.siemens.com/co/pool/hq/power-generation/power-plants/csp/solar_fresnel_large.jpg
[11] http://www.abengoa.com/export/sites/abengoa_corp/resources/pdf/noticias_y_publicaciones/presentaciones/20130904_CSP-Parabolic_En.pdf

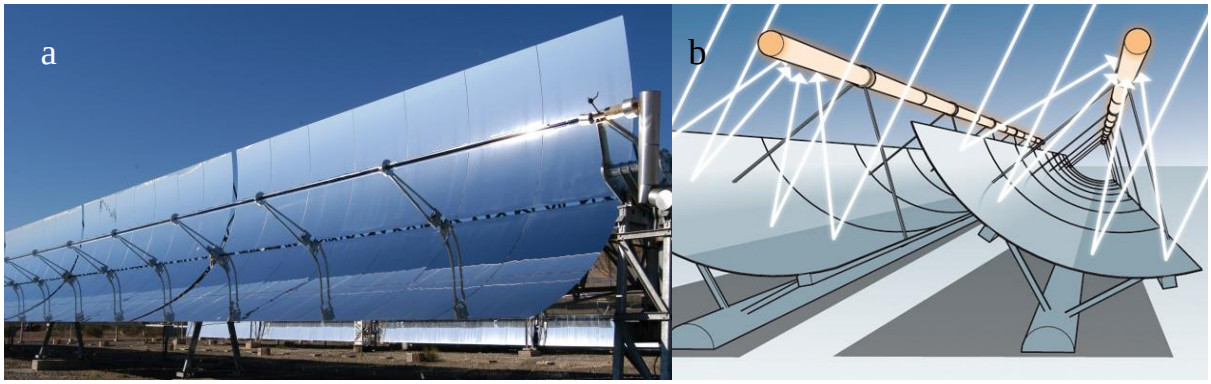

Fig. 1.6 Parabolic trough collector, (a) Photograph[12], and (b) Schematic diagram[13]

In the conventional system of the parabolic trough collector system, there is reflector, known as the parabolic trough. The reflector reflects all the solar irradiation on its focal line, and on the focal line a receiver is placed. The receiver is composed of a selectively coated absorber tube (having high absorptivity in the solar irradiation wavelength band and low emissivity in the infrared region), enveloped by transparent low iron glass tube. Glass envelope is used to reduce the convective losses. With the use of glass tube, optical efficiency of the system is effected by a small amount but comparatively large gain is achieved in the thermal efficiency. This happens because of the reduction in the convection losses by the great amount. There comes a number of possibility, there could be any gas in the annulus. The vacuum has the highest thermal efficiency and the hydrogen gas has the least efficiency if used in the annulus (Forristall, 2003). The hydrogen gas being the lightest gas has the maximum convection currents in the annulus leading the maximum rise in the temperature of the glass envelope. On the other hand when we use the vacuum in the annulus the convection currents are least, leading to negligible rise in the glass envelope temperature. Hence the system with vacuum in annulus has the highest thermal efficiency and least convective losses. The glass envelope being typically made up of low iron glass renders it high transmissivity (approx. 95%) in the incident solar irradiance wavelength but high absorptivity in the mid-infrared region (Khullar, 2015 and Dudley et al., 1995). The latter optical characteristic results in high radiative losses as the receiver temperature rises.

Now, due to the geometry of the system, the receiver side facing the trough will have high concentrated flux, compared to the remaining portion. So basically the heat flux distribution around the receiver tube is non-uniform, only a limited portion of the receiver receives concentrated solar irradiation (Jeter, 1986; Jeter, 1987 and Galindo and Bilgen, 1984).

[12] http://www.dlr.de/dlr/en/Portaldata/1/Resources/bilder/portal/portal_2011_2/solartechnik2.jpg
[13] http://www.energy.siemens.com/co/pool/hq/power-generation/power-plants/csp/solar_parabol_large.jpg

However, the receiver has thermal losses from all over the circumferential area. Therefore, in order to improve the efficiency of the collector, a mechanism needs be devised to reduce the circumferential area from which thermal losses take place without hampering the optical efficiency of the system. In previous years, numerous researchers have attempted to engineer modifications in the conventional parabolic trough design which could either improve the flux distribution or instead take advantage of the non-uniform flux distribution around the receiver to improve the overall efficiency of the parabolic trough collector.

More recently in 2011, Ansary and Zeitoun, engineered a mechanism (in case air filled annulus receivers) to minimize the thermal losses (particularly, convective losses) by filling a portion of the annulus by fiberglass insulation. However, it was found that such design modification were beneficial only for low receiver temperatures as the losses increase when the working temperature increases.

1.5 Novel design idea

The present study introduces the idea of using transparent heat mirrors, instead of using insulation in the annulus, a coating of the Sn-In_2O_3 is done, which will act as a heat mirror. Heat mirror has the special optical properties, it allows the incident solar irradiance to pass through but reflects back the radiant energy emitted by the absorber tube (in the wavelength range of 2µm - 10µm). The coating has transmissivity of 0.85 in the solar irradiation wavelength band (Khullar, 2015). Hence, effectively reducing the thermal losses, without significantly hampering optical efficiency.

In case of the conventional receiver design, optical losses are inherently low owing to the usage of low-iron glass envelope. However, in the proposed receiver design, optical losses increase with increase in the circumferential heat mirror angle. But at the same time, both the radiation losses and the convection losses dip down significantly, especially at higher temperatures. Since the system which is considered in the present study has 70^o rim angle, the major local concentration is up to 180^o of the receiver towards the trough (He et al., 2011 and Jeter, 1987). Solar irradiation gain on the upper 180^o is essentially one sun only. However, the thermal loss takes place from the entire circumference. Therefore, the upper half portion of the receiver could be coated so as to act as a heat mirror and reduction in thermal losses could be realized.

The present study essentially presents a detailed heat transfer model pertinent to such novel solar thermal systems which employ a hybrid envelope configuration (a portion of the glass envelope is coated so as to act like a heat mirror) to minimize thermal losses without affecting the optical efficiency of the system.

1.6 Thesis Objectives

- To build a detailed heat transfer model pertinent to heat mirror based parabolic trough receiver design.
- To assess the performance of such novel receiver design.
- To identify the most critical operating and design parameters which significantly affect the performance of such systems.

Chapter 2

Literature Review

2.1 Introduction

In the starting of this chapter, the basic geometry of the conventional PTC system is explained with its working principle. Through rigorous literature review, several geometric and operating factor which effect the performance of the system have been identified. Subsequently, the most critical factor in the present framework i.e. heat flux distribution has been discussed in detail. Finally how heat mirror can be put to use for taking advantage of non-uniform flux distribution has been presented.

Parabolic trough collector (PTC) system has a reflector which is called trough, it has high reflectivity. All the solar irradiation which fall on the trough is reflected onto the receiver tube. Due to geometric property of the trough shape (parabola), all the reflected irradiation are concentrated onto the focal line. At the focal line a selective coating metal tube is placed which absorbs the solar irradiation and transfer this heat to the heat transfer fluid. Now the fluid which is passing through the tube is called the heat transfer fluid (HTF). It can be any fluid, but it is required to be selected in accordance the with operating temperature range, like if the system is used for domestic purpose and the temperature limit is below 100 °C, then water is the best option and if the temperature limit extends beyond 100 °C, then synthetic oil could be the right choice. Now to reduce the thermal losses from the system, a glass envelope is used. First, it restricts the direct exposer of the high temperature metallic tube to the environment and second, it controls the thermal losses. Envelope is generally used which is made of low iron glass [having high transmissivity for solar irradiation in the solar band width (0.2-2.5 μm)]. The HTF after getting heat from receiver, is used where heat is required, it could be for domestic purpose like water/air heating or for the generation of the electricity, it could be stored in the thermal heat reservoirs. Now the thermal losses depends very much on the gas used in the annulus, it could be air, inert gas, hydrogen gas, or low pressure air (vacuum). Vacuum configuration results in maximum thermal efficiency among all the aforementioned options because of the least convection losses. When there is very low pressure in the annulus then the convection current is least effective compared to the normal pressure filled gas in the annulus. So when there is vacuum in the annulus then mainly there are radiation losses and the convection losses are negligible. The thermal efficiency of the system depends upon a number of factors, it could be operating parameter such as wind speed, mass flow rate of the HTF, or geometric properties

of the system such as length, width. Therefore, a detailed literature review has been carried out to identify the most critical parameters.

2.2 Design and operating parameters

2.2.1 Effect of geometry

Effect of length (L)

As the length of the receiver is increased, the time for the HTF to gain the energy increases, that's why the outlet temperature of the HTF increases. There is an optical loss, called as the end loss effect. It happens normally in stationary or single axis tracking system. For the solar irradiation coming at non-zero angle of incidence, there is always a small portion facing towards the sun, which never gets the concentrated heat flux on the receiver, and some portion of concentrated heat flux goes in waste through the opposite edge, this is called end loss effect. It was found that as the length of the receiver is increased, the gain in temperature of the HTF increases (Xu et al., 2014). Furthermore, as the length is increased, the non-uniformity in the axial direction decreases, and hence end loss effect decreases. For the receiver length less than 15 meter (W=3, fl = 1.2), the end loss effect have significant role (Xu et al., 2014). It was suggested by Xu et al., 2014, that for the receiver having length less than 15 meters, a mirror can be used at the other edge of the receiver, which will reflect back the solar irradiation on the trough and again be reflected back to the receiver, it will increase the efficiency of the system (Xu et al., 2014).

Effect of the rim angle (ψ)

As the rim angle is increased, the geometric concentration ratio is increased, which further leads to the non-uniform heat flux distribution in the circumferential direction. The non-uniform heat flux was calculated by Tomas and Guven, 1994, and they found that when the rim angle was changed from 92° to 52° the concentrated flux essentially circumscribes the lower half of the receiver tube. Furthermore, when the rim angle is held fixed and the concentration ratio is increased then the lower half of the receiver tube gains more flux distribution (Thomas and Guven, 1994).

He et al. in 2011 carried out, a coupled simulation in which MCRT and FVM were coupled, and they found that as the value of the rim angle was increased beyond a certain value, the maximum value of the heat flux went down. Furthermore, it was reported that the heat flux distribution is heterogeneous in the circumferential direction but homogeneous in the axial

direction (He et al., 2011). The heat flux distribution around the absorber tube could be divided in four regions, first is shadow effect region, second is the heat flux increasing region then third is the heat flux decreasing region and the fourth is the direct beam irradiation region (Cheng et al., 2014; He et al., 2011; Wang et al., 2015; Thomas and Guven, 1994; Yang et al., 2010; Jeter, 1986 and Jeter, 1987). (See Fig. 2.1)

For 'W'<15 m, If the rim angle is small (ψ <30°) then the first and second region tend to become less pronounced, as ψ is increased, then second region start to come into picture, 30°< ψ <60°, then further increase in the ψ leads to a flux distribution in which all the four aforementioned regions are present. (See Fig. 2.2). However, for 'W'>15 m, the heat flux distribution pattern changes slightly and difficult to describe in four regions. This is because the absorber tube starts missing the concentrated reflected beams (Cheng et al., 2014).

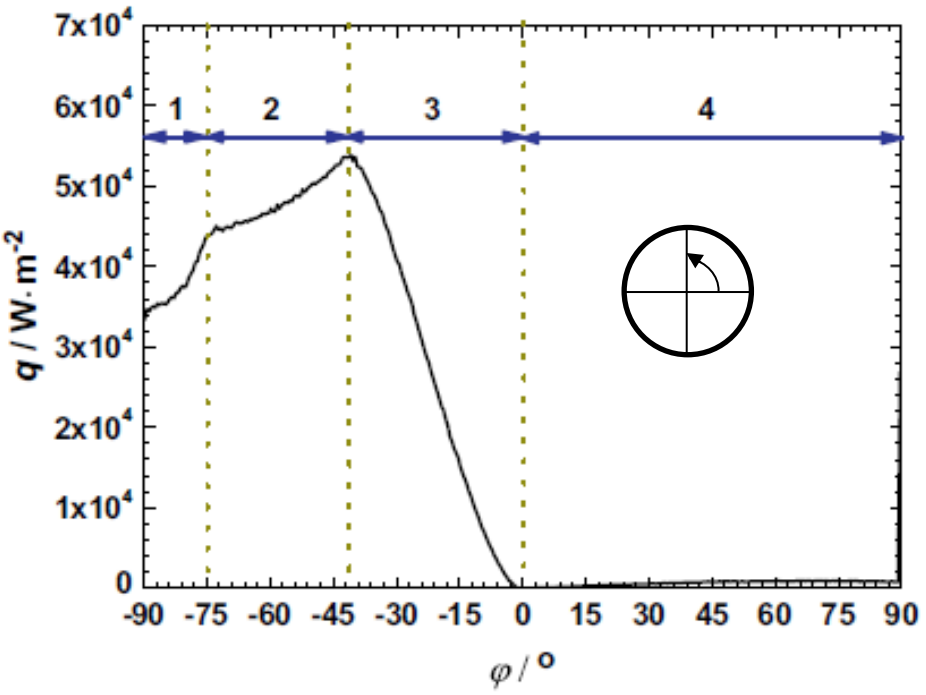

Fig. 2.1 Concentrated heat flux distribution around the receiver tube with different regions (data point taken from Ref. Jeter, 1986).

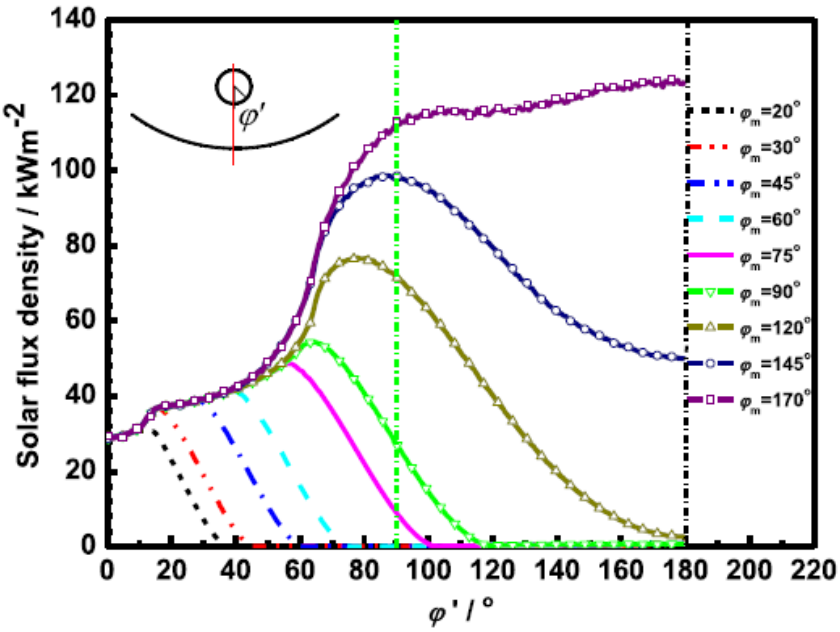

Fig. 2.2 Variation in solar flux distribution with rim angle for constant focal length (Cheng et al., 2014).

Effect of aperture width (W)

Aperture width of the PTC is an important geometric parameter that determine in the performance and the structural stability of the system. As the aperture size (width) is increased, the concentration ratio increases (Paetzold et al., 2014). As discussed earlier, the heat flux distribution around the receiver tube can be divided in four regions, and as the aperture width (W) is increased, the width of the 2nd and 3rd region tend to increase (Cheng et al., 2014). It was found by researchers that for the aperture width of 1.5 to 24 meters, 1st region (shadow region) remains in the range of 15-20° (see Fig. 2.2), it was found that as the aperture width is increased, the geometric concentration ratio also increases and because of that the peak value of the heat flux around the receiver tube also increases, at the same time the area under the curve also increases (See Fig. 2.2) (Cheng et al., 2014).

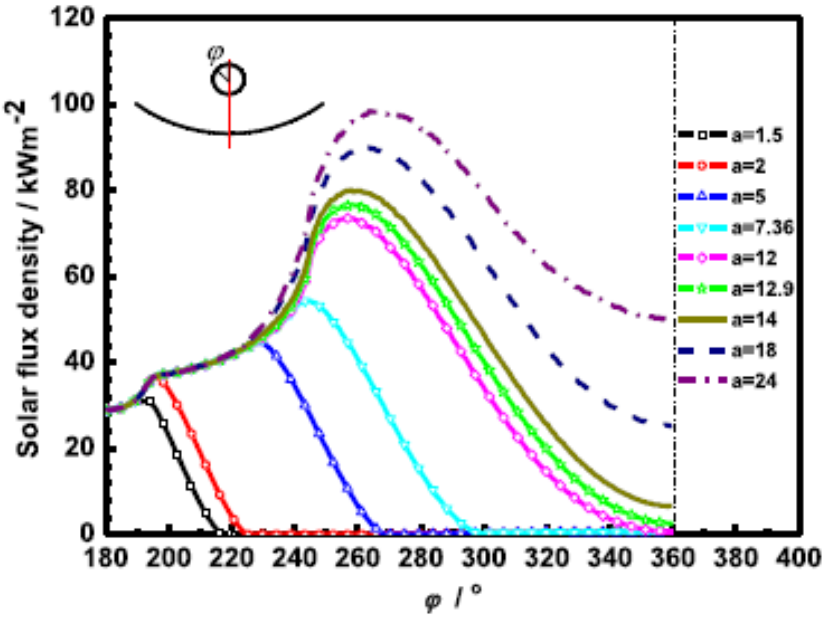

Fig. 2.3 Heat flux distribution around the receiver tube with varying aperture width

(Cheng et al., 2014)

It is easily understandable that when the aperture width is less than 2 m, then the 2nd region decreases, it happens because this region is unable to receive the irradiation owing to decrease in the reflective surface area. As it is visible that if the aperture width is increased beyond a certain value, there will be gain in performance, however when the 'W' is increased, there comes a factor of structural stability. Because when such system is used practically then it has to face wind loads also. And that's why, both the factor have to be taken into consideration while deciding the aperture width.

Effect of focal length (fl)

Now with the aperture width, there is one more factor, which is quite related to the same. That is the focal length (fl) of the parabolic trough. As shown in the Fig. 2.1 and 2.3, for the constant aperture width, the area under the curve is constant just the region interchanges the shared area. As the focal length is increased the first and the fourth region increases. Cheng et al., 2014 found the effect of focal length, focal length was varied in between 0.1-4.64 meters. However, for $fl < 0.75$ m, shadow region does not exist. In other words, $fl = 0.75$ m marks the onset of the shadow region. Therefore, it can be only divided in four region (See fig. 2.1). But this trend doesn't hold for all ranges of the focal length (See fig. 2.3). As discussed earlier that for a constant rim angle, area under the curve is constant. Therefore as we increases the fl

the curve shifts toward the left side. As fl is increased beyond 2.24 m, the first region (shadow region) and the second region (solar flux increasing region) begins to disappear. Furthermore, if the focal length is chosen such that it becomes equal to or greater than the receiver outer diameter, then the defocusing phenomenon starts (See fig. 2.4).

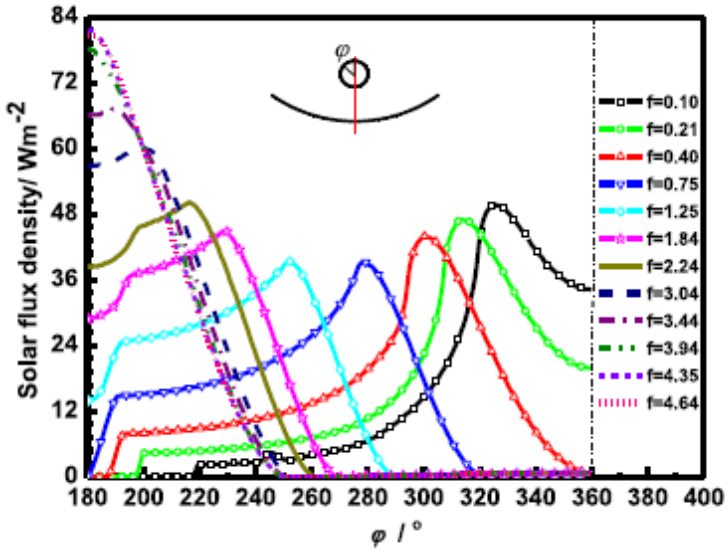

Fig. 2.4 Concentrated heat flux distribution around absorber tube for focal lengths ranging from 0.1 to 4.64 m (Cheng et al., 2014).

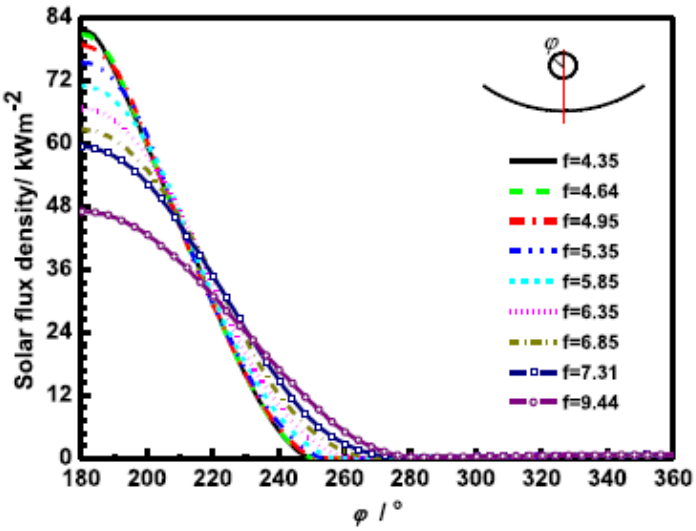

Fig. 2.5 Concentrated heat flux distribution around absorber tube for focal lengths ranging from 4.35 to 9.44 m (Cheng et al., 2014).

One more factor, which can be the deciding factor for the focal length, is the structural stability. If too deep trough is used, then it leads to higher wind loads and even this could topple the trough due to generated pitching moment. However, deep trough causes the sheltering effect, as the speed of the wind blowing over the receiver goes down, which lead to decrease in the convection losses. Therefore, deeper troughs have inherently high thermal and the optical losses. As the depth of the trough is increased the edge portion of the rim starts reflecting back the incident solar irradiation, which leads to the defocusing phenomenon, and hence reduction in optical efficiency. Furthermore, deep trough always leads to the higher instability of the parabolic trough under wind loads compared to the shallow trough (Paetzold et al., 2014).

Effect of pitch angle

For the pitch angle of less than 15°, and greater than -60°, wind exerts higher forces on the trough. As it is well known, that the PTC systems are arranged in a row so in the discussed range of the pitch angles, wind possess large eddies behind the trough, and which leads to compromise with the efficiency and the structural stability of the PTC system (Paetzold et al., 2014).

2.2.2 Operating parameters

Effect of geometric concatenation ratio (GCR)

When the geometric concentration ratio is increased, it leads to increase in the solar heat flux incident on the receiver. When the GCR increases, the spreading of the concentrated rays goes mainly at the bottom of the receiver tube (See fig. 2.5), (Thomas and Guven, 1994). It was concluded by the researchers that the effect of GCR is only in the circumferential direction, and that generated region can be divided into four regions as discussed earlier (Thomas and Guven, 1994; Khanna et al., 2014; Cheng et al., 2014; He et al., 2011 and Jeter, 1986). There is no such effect on the axial direction, and as the length of the PTC trough is increased, heat flux distribution become gentler (He et al., 2011). With rise in GCR, the thermal efficiency of the system also increases (Manikandan et al., 2012), at the same the rise in HTF temperature increases (Arasu and Sornakumar, 2006).

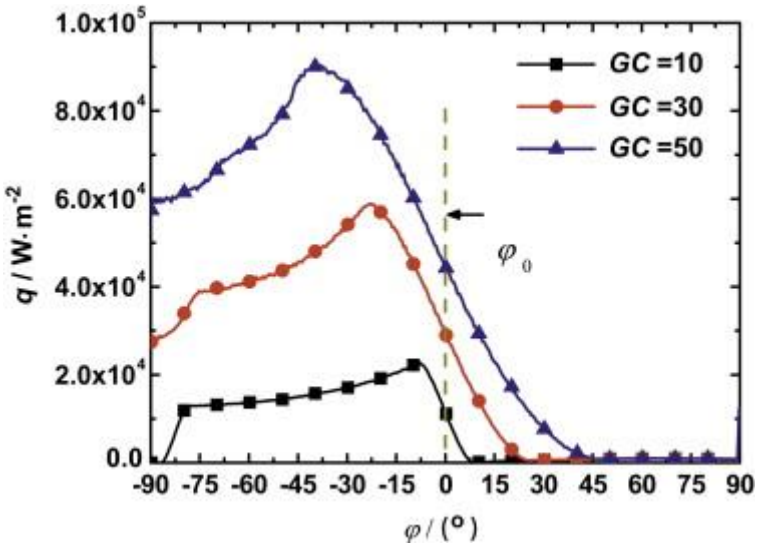

Fig. 2.6 Heat flux distribution under different GCR on circumferential direction

(He et al., 2011)

Effect of solar irradiation (S)

The effect of solar irradiation is quite obvious on the performance of the system. As the day is more sunny, it will bring more 'S', and this results in the enhancement of system efficiency. This is because the amount of useful energy gain increases resulting in higher temperatures (Manikandan et al., 2012). With the increase in 'S', the circumferential temperature difference (CTD) of the receiver tube increases (Wang et al., 2015).

Effect of angle of incidence

Incident angle of solar irradiation is a critical parameter in determining the optical efficiency of the system. It is desirable to have normal angle of incidence (Jeter, 1987).

Effect of mass flow rate of heat transfer fluid (m_f)

With increase in m_f, there is a rise in the thermal efficiency of the system, because more water will come in contact to gain same amount of energy in the same time, there will be less heat transfer coefficient for the less m_f (Manikandan et al. 2012 and Yilmaz and Soylemez, 2014).

With increase in m_f, the circumferential temperature difference (CTD) of absorber decreases (Wang et al., 2015).

Effect of wind speed (v)

This is quite obvious that, with the rise in wind speed the thermal losses will also increase. Even when the system is in no wind condition, there will be some convection loss too. There will be some air blowing around the receiver tube, and increase in the air speed will lead to increase in the convection losses from the receiver tube. At low absorber temperature, basically the effect of the wind speed predominately depends upon the gas in the annulus, if it is the vacuum, then the change in losses would be minimum, and as same for air will depends too much on the wind speed (Tijani and Roslan, 2014 and Yilmaz and Soylemez, 2014).

As air velocity or wind velocity (v) increases, the thermal losses increase therefore the efficiency of the system goes down. The system having vacuum in annulus is more efficient than the system having air in the annulus (Yilmaz and Soylemez, 2014).

The main effect of the higher wind speed is on the structural stability of the system. When wind blows then depending on the aperture width and rim angle, wind load is generated. There is a quadratic relationship in the wind speed and forces generated due to wind load (Zembler et al., 2013).

$$F(x,y) = C_o v + C_1 v^2 + C_2 W + C_3 W^2 + C_4 vW \qquad \text{(Zembler et al., 2013) (2.1)}$$

here, $C_0 - C_4$ are constants, v is the wind speed and W is the aperture width.

If there is a deep trough, then the wind load have significant effect on the structural stability (Paetzold et al., 2014).

Effect of HTF inlet temperature ($T_{\inf}$)

If the inlet temperature of the HTF is increased, then the thermal losses of the system increases, which is quite obvious because the operating temperature of the system increases. Hence with the rise in the thermal losses, the efficiency or the performance of the system predominantly decreases. Furthermore, it may be noted that thermal losses escalate mainly due to increase in radiation losses. It is always favourable to have the high heat transfer rate at low pressure drop from the economic point of view. Now, increase in HTF temperature is favourable as the average friction factor for the flow decreases (Cheng et al., 2012). However, a theoretical investigation by Manikandan et al., 2012, concluded that with the use of high inlet temperature of the HTF, the useful energy gain goes down. In other words, if the inlet temperature is higher,

then the rise in temperature will be less so the useful energy goes down. Hence, overall the thermal efficiency decreases with increase in inlet fluid temperature.

Furthermore, when the high temperature HTF is sent to the system, then its mean bulk temperature increases, which leads to the thermal deformation of the receiver tube, but the CTD of the receiver tube goes down. As it was found out that the thermal deformation of the metal tube and glass tube is different and the deformation of metal tube is more than the glass tube. For this combined study of fluid flow with heat transfer flow along with the thermal stress, was done by Wang et al., 2015.

Effect of annulus gas

As it is known that to reduce the thermal losses, a glass envelope is used. Now there comes a region called as annulus in between the outer surface of metal tube and the inner surface of the glass tube. Now theoretically there can be used any substance but due to practical limitation there is only a number of possibilities such as, air, vacuum or any inert gas as argon.

For different flow conditions and for different selective coatings, on-sun and off-sun case, results were evaluated by Padilla et al., 2011, and it was find out that, the system having vacuum in the annulus, gives maximum efficiency.

A numerical simulation was carried out with a three dimensional model, coupling of finite volume method (FVM) with Monte-Carlo ray trace method (MCRT) by Cheng et al., 2012. The maximum efficiency was observed in the case of vacuum followed by argon gas and air in annulus. It was also found that Therminol VP1 and Syltherm 800 give better results than Nitrate salt or Hitec XL, because the PTC system operates at higher temperature (above 150 °C) and at such temperature the average Nusselt number increases as the inlet HTF temperature increases, which causes the increase in heat transfer rate (Cheng et al., 2012). Theraminol VP1 and Syltherm 800 have higher rise in average Nusselt number than Nitrate salt or Hitex XL.

As the wind speed increases, if there is vacuum in the annulus then thermal losses are affected in very small amount as compared to the air in the annulus case, but this effect for air in annulus also decreases when the mean bulk temperature reaches 150 °C (Yilmaz and Soylemez, 2014).

Non-Uniform heat flux distribution (HFD)

In 1986, Jeter found that the incident solar heat flux on the parabolic trough is not uniform. Later on by extending the same work, Jeter, in 1987, found that the non-uniformity is only in the circumferential direction and it is uniform in the axial direction. In the same work of Jeter,

several factors were taken into consideration like the effect of geometry, incident angle, and shadow effect.

Heat flux distribution (HFD) is directly dependent on the rim angle, if the ψ is shifted from 92° to 52° then it shifts mainly towards the lower half portion of the receiver tube. It is quite obvious that the concentration ratio will have the direct effect on the heat flux distribution, with the increasing value of GCR, spreading of the solar irradiation goes mainly in the bottom area of the absorber (Thomas and Guven, 1994).

With the help of MCRT method, Heat flux distribution was calculated by Yang et al, 2010. A probability model was used and the results were compared with Jeter, 1986. It was a good alternative method to calculate the heat flux distribution.

The effect of rim angle and GCR is calculated with the help of coupled simulation in which MCRT and FVM are used by He et al, 2011. With increasing GCR, HFD become gentler. With increasing ψ , the peak value of HFD decreases.

Detailed study of parameters of the PTC was done by Cheng et al., 2014. A three-dimensional model was evaluated with the help of coupled simulation in which FVM and MCRT was used. The effect of various factors like effect of 'W', fl and ψ , on the heat flux distribution, have already been discussed.

The effect of non-uniform heat flux distribution on the thermal stresses was evaluated with the help of solar ray trace method (SRT) and Finite element method (FEM), by Wang et al., 2015. It was found that the temperature profile for envelope and absorber tube is quite similar, but the deformation happening because of high temperature is more in metal than glass tube. With the rise in solar irradiation (S), CTD also increases. With the higher HTF inlet temperature CTD of absorber decreases, the reason already have been discussed. Now, a more related phenomenon that is bending of absorber tube can be discussed. Because it is directly related to the combined effect of HFD and end loss effect. When end loss effect occurs then the probability of the bending of the receiver tube increases due to thermal stress induced in the receiver. End loss effect mainly occurs when the solar irradiation is not normal to the trough reflector. At the same time if the rise in HTF temperature is high, then it also leads to bending, higher the difference in inlet and outlet temperature, higher will be the deflection (Khanna et al., 2014). As the thermal deformation of metal is more compared to glass tube (Wang et al., 2015), hence it is required to take into consideration the annulus gap. But with the increase in

the annulus gap also leads to compromising with the performance of system, which is easy to understand. For higher annulus gap, it is required to have higher outer diameter too of the glass envelope, which gives more surface area to lose energy, hence the thermal losses increases (Egbo et al., 2014)

2.3 Relevance of heat mirror in reducing thermal losses

Low-e glass can't be used in the PTC system directly, because of its optical properties. It only allows the visible region of the solar irradiation to pass through it and reflect the infrared region, which is nearly about 50% of the energy at concentrated solar irradiation (Taylor et al., 2016). So a selective coating on the glass envelope can replace this problem.

Heat mirror use in the field of the PTC collector is relatively new concept, some researcher have tried to do work on the selective coating on the glass envelope to behave like a heat mirror. Some layers of the specified substance is coated on the glass envelope so that it gets the specified required optical properties. The concept of coating on glass envelope is of worth only when the operating temperature is high and radiative losses are high, i.e. for system having glass temperature more than 100 °C, the selective coating on the glass is used, otherwise it would be useless and will have negative impact on the performance of the system (Taylor et al., 2015). Because radiation loss is proportional to four power of temperature, and at high temperature, the radiation losses increases dominantly. At low temperature, radiation losses is less as compared to convection losses.

A glass envelope behave like the heat mirror if coating is done on it. It could be possible by two means. That could be semiconductor based or the metallic film based. It should have high transmissivity in the solar irradiation wavelength band and low emissivity in the mid infrared region.

2.3.1 Mechanism or the working principle of heat mirror

To make the glass envelope behave more likely the heat mirror, it should have the desired optical properties, which are, it should allow most of the visible-non-infrared radiation to transmit through it, this will lead to the phenomenon of transmitting the most of the solar irradiation through the heat mirror, and second is, it should be highly reflecting in the infrared radiation wavelength band. To achieve the good reflectance in the infrared-radiation region, it should have enough amount of the free electron/hole pair concentration. This could be achieved by two ways, either by the highly doping of the semi-conductors, which are coated by the

selective antireflective coating. And the second way is, there can be an ultra-thin metallic film which is being sandwiched in-between the layers of the selective coating, selective coating are the antireflective coatings (Khullar, 2015).

Semiconductor based heat mirrors

In this type of heat mirror, there are primarily two parameters, which governs the desired optical properties. The first one is the electron/hole concentration, which means how much doping is done, and the second one is the film thickness. As the concentration of the electron/hole is increased, it moves towards the reflectance of the shorter wavelength, which comes in the region of the solar irradiation, which is not desired. This phenomenon can be explained by the increase in the amount of the doping result in increase in the electron/hole concentration, which leads to increase the inter-band transitions, which basically increase the infrared region's reflectivity. Now, the second factor is the thickness of the film, it should be as thin as possible to confirm the high transmissivity for the visible-non-infrared radiation, however, if the film thickness is below a critical level, then the reflectivity of the infrared radiation tends to decrease. So basically both factors are interconnected, and for the specific application, both the parameter should be taken care of (Khullar, 2015).

Metal film based heat mirrors

As the desired optical property is to have solar irradiation wavelength band to transmit through envelope, it is possible by the help of very low thickness and at same time with the right choice of the metal. Some metal behaves in the favour and some do not, so metal selection is also required. For the case of the Nobel metal, there is free electron which governs the high infrared reflectivity (Fan and Bachner, 1976 and Fan et al., 1974) as discussed earlier. $TiO_2/Ag/TiO_2$ does not show the desired optical property of high visible-non-infrared transmittance because of its spectral transmittance curve, but on the opposite, spectral reflectance and transmittance curve for Sn-In_2O_3 based heat mirror, which are semiconductor based heat mirror has high desired optical property (Khullar, 2015).

Many researcher have worked on the selective coating of the envelope to make it behave like the heat mirrors. $TiNO_X$, Black-chrome are used for the coating on the absorber (Taylor et al., 2015 and Taylor et al., 2016), it ensures the high absorptivity in the selected wavelength region but it also emits radiation in the other selective radiation and at high temperature the radiation losses becomes the major loss factor. $TiNO_x$, uses several layers which are very thin, of vapour deposits (ceramics and metal) on the metal absorber tube. It makes the ratio of solar absorption

to thermal emission up to 20 (Taylor et al., 2016). So to enhance the performance and lower down the radiation losses, glass envelope is coated so that it can behave like the heat mirror. There is a technology of low-e glass, which allows only the visible region to pass through it, which leads to 50% loss of the radiation (Taylor et al., 2016). The other technology is to have optically layer of metal oxide over the substrate, which is very difficult to fabricate. So a fabrication was tried by Taylor et al., 2015, in which a low cost alternate solution was provided by the thin film of the coating of the transparent conducting oxides. A deciding factor was selective to the efficiency factor for selectivity (EFS), on the basis of this factor, ranking was done for several combination. It was concluded that the indium oxide (ITO) and ZnS/Ag/ZnS is best for the selective coating on the glass envelope (Taylor et al., 2015 and Taylor et al., 2016). In both of them ZnS/Ag/ZnS has more preferable properties but since ITO is easy to fabricate so it is much better than the ZnS/Ag/ZnS (Taylor et al., 2016). At a given incident angle the best dielectric material is ZnS followed by Al_2O_3 followed by TiO_2 (Taylor et al., 2015). For metals, 'Ag 'has lower absorption and refractive index in the solar spectral regions, which results in the high transmittance of the visible-non-infrared region. 'Al' has high reflectance than 'Au' and 'Cu', this is the region that ZnS/Ag/ZnS is best among all the selective options. (Taylor et al., 2015). For the transparent conducting oxide layer type ITO is better than the FTO and AZO, FTO and AZO are supposed have same preference (Taylor et al., 2015).

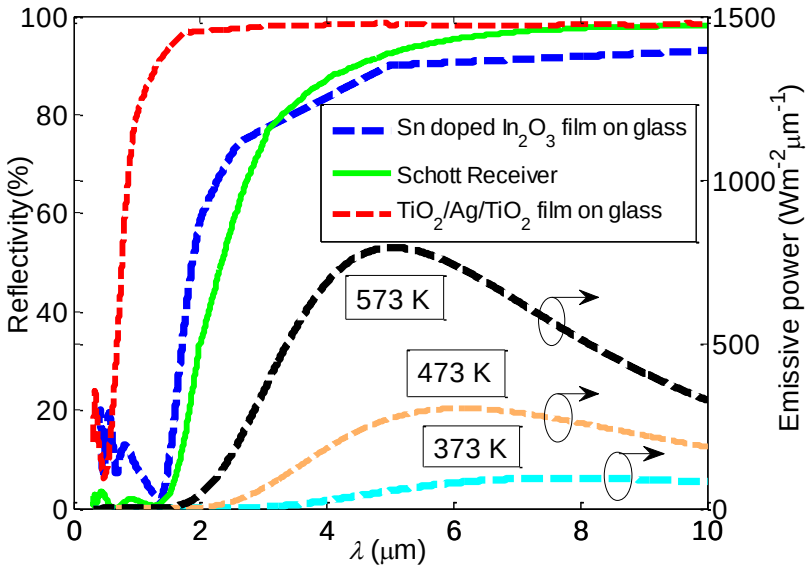

Fig. 2.7 Optic properties of different selesctive coating (Khullar ,2015)

2.4 Utilization of non-uniform heat flux distribution

Several attempts have been made to take advantage of the non- uniform heat flux distribution. Recently, in 2011, an alternative design was proposed by Ansary and Zeitoun, 2011, in this it was suggested to use the insulating material in the upper half annulus, taking into consideration that the major heat flux remains in the lower half the receiver. But the use of the insulation in the upper half does not solve the issue at higher temperatures, the conduction losses starts to come into picture, hence the performance of the system goes down at high temperatures. Hence, it is not a good alternative design especially at higher temperatures.

In 2014, Yilmaz et al., studied the effect of annulus material and generated a mathematical model. Because vacuum gives best results from the thermal efficiency point of view but it is costly, so for the air in vacuum, later on it was suggested that there can be low conducting heat transfer fluid droplets to lower down the convection losses compare to system having air only in the annulus. But it could lead to the accumulation the fluid droplets at the bottom region of the tube, which is not preferable.

In the present study, instead of using any gas or fluid droplets in the annulus, vacuum is considered with $Sn\text{-}In_2O_3$ coating on the glass envelope, the coated portion behaves like a heat mirror owing to its high reflectivity in the mid infrared region and fairly reasonable transmissivity in the solar irradiation wavelength band. The former critical characteristic ensure low radiation losses as discussed in the following chapters.

Chapter 3

System Design and Modelling

3.1 Introduction

First of all the geometric difference in the conventional and the proposed receiver design is elaborated. Subsequently, the formulation of the one-dimensional heat transfer model is detailed. Furthermost, the governing equations based on optical and overall energy balance have been presented. Finally, these governing equations have been solved through an algorithm from implemented in MATLAB (R2010b).

3.2 Basic design and constructional details

The proposed receiver design is similar to the conventional receiver design (See Fig. 3.1(a)) except for the envelope part. As in conventional PTC receiver, there is parabolic trough, which is used to concentrate all the incoming solar irradiation onto the receiver tube which is made of the high conductive metal tube coated with some selective coating having special optical properties like the high absorptivity in the solar irradiation region and low emissivity in the infrared radiation band width of the wavelength. To minimise the thermal losses, a glass envelope is used. With the help of the glass envelope, the convection current around the receiver tube goes down hence the temperature of the system having direct contact with the environment become lesser therefore the thermal losses are less as compared to the bare metal tube. Now further there comes a number of possibilities like there could be gas or vacuum in the annulus. The system having vacuum in the annulus has the maximum efficiency and the minimum thermal losses. When there is vacuum in the annulus then the convection current in the annulus is minimum and the major heat transfer losses takes place via radiation mechanism. Now because of the non-uniform heat flux distribution, the concentrated heat flux has a limited access to the angular region of the receiver tube. Therefore the gain is not uniform around the circumference of the receiver, but the losses occurs across the entire circumference. It is possible to use non-uniform heat flux distribution, like there is the possibility to have a small compromise with the optical efficiency with a great decrease in the thermal losses. For this, some portion of the low iron glass envelope is coated with Sn-In_2O_3 (See Fig. 3.1(b)). Therefore, the envelope could be combination of two parts: uncoated and the coated part. This hybrid cover ensures high transmissivity in the solar irradiation wavelength band and low emissivity (high reflectivity) in the mid infrared region.

As previously mentioned, the uncoated part being made up of low-iron glass has high transmissivity (approx. 95%) in the incident solar irradiance wavelength band and high emissivity in the mid-infrared region. On the other hand, the coated part has relatively lower transmissivity (approx. 85%) in the incident solar irradiance wavelength band. but at the same time has high reflectivity in the mid-infrared region. Thus, the two aforesaid characteristics can be exploited to make a sort of hybrid envelope having coated and uncoated regions depending upon the solar irradiance flux distribution around the receiver. This design shall ensure reduction in radiative losses (especially at high receiver temperature) without significantly affecting the optical efficiency of the system.

Note: In the present study, the proposed novel parabolic trough design has dimensions similar to that described in Dudley et al, 1995. Furthermore, Table 1 details the optical properties of various components of the parabolic trough.

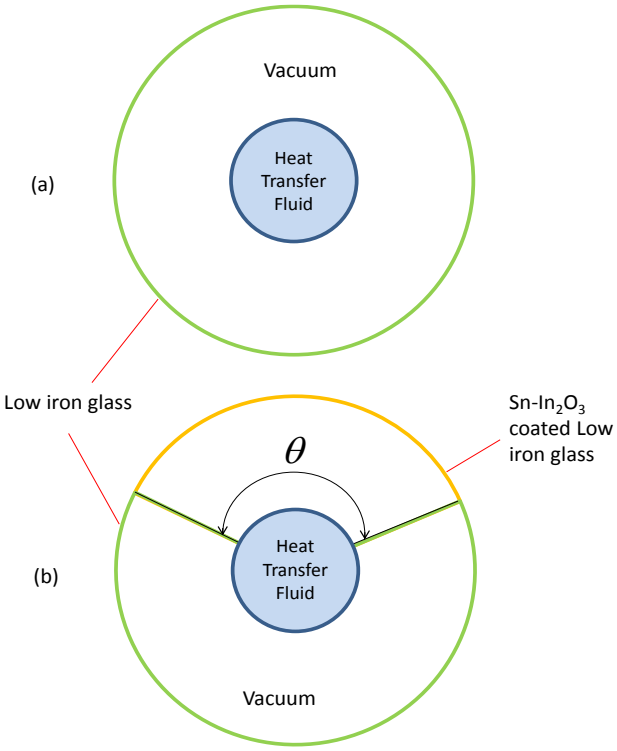

Fig. 3.1 Schematic showing comparison between conventional and proposed parabolic trough receiver designs

3.3 Theoretical formulation

The proposed model is based on the energy balance, which is applied on the energy incident on the parabolic receiver and the losses occurring through it. The schematic of the proposed receiver design is illustrated in the Fig. 3.2. Solar irradiance which is incident normally on the

parabolic trough aperture is focused onto a cylindrical receiver lying along the focal axis of the parabola (see Fig. 3.2 a). Depending on the optical properties of the glass envelope, a small portion of the incident solar irradiance is reflected/absorbed by the glass envelope and rest (majority about 95%) is able to reach the selectively coated metal tube. Here, the radiant energy is converted into the thermal energy gain in the metal tube (depending on the absorptivity of the selectively coated metal tube, in the present study, $\alpha = 0.96$). Finally, the thermal energy in the metal tube is transferred to the working fluid primarily through forced convection mechanism (See Fig. 3.2(b)).

Table 3.1. Optical Properties of various components of the parabolic trough collector (in specific wavelength regions)

	Parabolic Concentrator	**Uncoated portion of the glass envelope**	**Coated portion of the glass envelope**	**Selectively coated metal tube**
Reflectivity	0.93 (averaged over solar irradiance wavelength band)	-	1 (averaged over the mid-infrared wavelength band, 2μm - 10 μm)	-
Absorptivity	-	-	-	0.96 (averaged over solar irradiance wavelength band)
Transmissivity	-	0.95 (averaged over the solar wavelength band, .2 μm – 2.5 μm)	0.85 (averaged over the solar wavelength band, .2 μm – 2.5 μm)	-

On the thermal losses front, the receiver emits in accordance with its emissivity. This emitted radiant energy is predominantly absorbed by the uncoated portion of the glass envelope, whereas the coated portion of the glass envelope essentially reflects it back to the receiver. Vacuum/low pressure air being present in the annulus ensures significantly low convective heat transfer from the receiver to the glass envelope. Finally, the glass envelope rejects heat to the surroundings/sky through convective and radiative modes of heat transfer (See Fig. 3.2(b)).

In Figure 3.2, A_1, A_2, B_1, B_2, C_1, C_2, D, E, and F are as follows:

A_1: Incident solar irradiance on the uncoated portion of the low-iron glass envelope.

A_2: Incident solar irradiance on the Sn-In_2O_3 coated portion of-the low-iron glass envelope.

B_1: Incident solar irradiance that is able to reach the receiver after passing through the uncoated portion of the low-iron glass envelope.

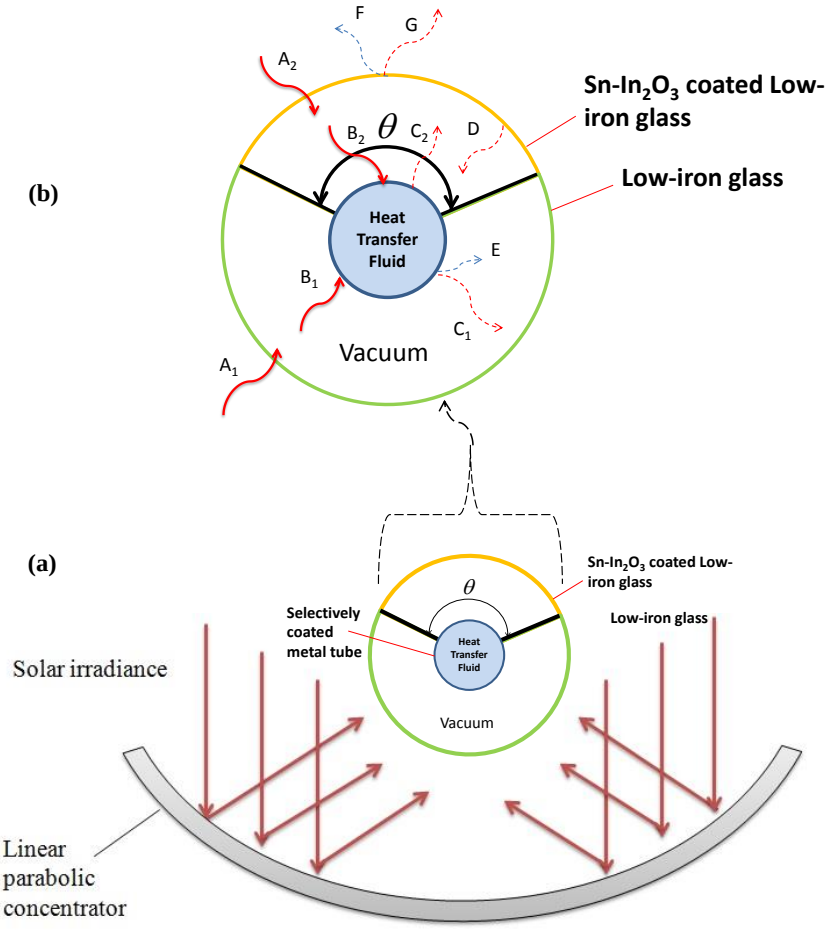

Fig. 3.2 Schematic showing a linear parabolic trough, 3.2 (a) Schematic showing a linear parabolic trough employing Sn-In_2O_3 based hybrid glass envelope, and 3.2 (b) heat transfer mechanisms involved in such receivers.

B_2: Incident solar irradiance that is able to reach the receiver after passing through the Sn-In_2O_3 coated portion of the low-iron glass envelope.

The sum of the B_1 and B_2 would be equal to the total amount of solar irradiation reaching to the receiver $\left(\bar{z}\right)$.

$$B_1 + B_2 = \bar{z} \tag{3.1}$$

C_1: Radiative heat transfer from the receiver to the uncoated portion of the low-iron glass envelope.

C_2: Radiative heat transfer from the receiver to the Sn-In_2O_3 coated portion of the low-iron glass envelope.

D: Mid-infrared radiations reflected from Sn-In_2O_3 coated portion of the low iron glass envelope back to the receiver.

E: Convective heat transfer from the receiver to the glass envelope.

F: Convective heat transfer from the glass envelope to surrounding.

G: Radiative heat transfer from the glass envelope to surrounding.

$$C_1 + C_2 - D + E = Q_{\text{loss1}} \tag{3.2}$$

$$F + G = Q_{\text{loss3}} \tag{3.3}$$

3.3.1 Underlying assumptions

Quantification of the heat transfer mechanisms necessitates some reasonable assumptions to be made. These assumptions have been carefully made so that the model remains sufficiently accurate for engineering purposes and captures the physics behind each of the heat transfer processes.

(a) Spectrally distributed solar irradiance has been assumed to incident normally to the aperture.

(b) Uncoated portion of the glass envelope has transmissivity of approx. 95% averaged over the solar irradiance spectral range (Dudley et al., 1995).

(c) Coated portion of the glass envelope has transmissivity of approx. 85% averaged over the solar irradiance spectral range. (Khullar, 2015)

(d) Effective sky temperature has been assumed to be 8° less than the ambient temperature (Duffie and Beckman, 1993).

(e) As in the present model, the trough length is less than 100 m; therefore, one-dimensional steady state heat transfer model gives satisfactory results (Forristall, 2003).

(f) Under steady state conditions, the amount of heat transferred from absorber tube to glass inner surface, then by conduction to outer surface, and then by outer surface to atmosphere is same.

3.3.2 Analysis

Optical energy balance

When the solar irradiation is incident on the parabolic trough then the most of the solar irradiation is reflected to the receiver tube placed along the focal axis. Hence the portion facing parabolic trough will experience more concentrated irradiation than the portion opposite to the parabolic trough. Therefore firstly, solar irradiance flux distribution around the receiver tube is essentially non-uniform (See Fig. 3.3(a)). Secondly, coated and the uncoated portions of the glass envelope have different optical properties like the absorptivity and the transmissivity. Finally, the amount of flux reaching the selectively coated metal tube is also dependent on the angle (θ) up to which the glass envelope has been coated (See Fig. 3.3(b)). As we increase the angle of the coating on the glass envelope, the amount of the solar energy incident on the receiver tube is correspondingly decreasing. Therefore, in order to compute the optical efficiency of the parabolic trough collector the three aforementioned factors should be considered in addition to the reflectivity of the concentrator and absorptivity of the selectively coated metal tube.

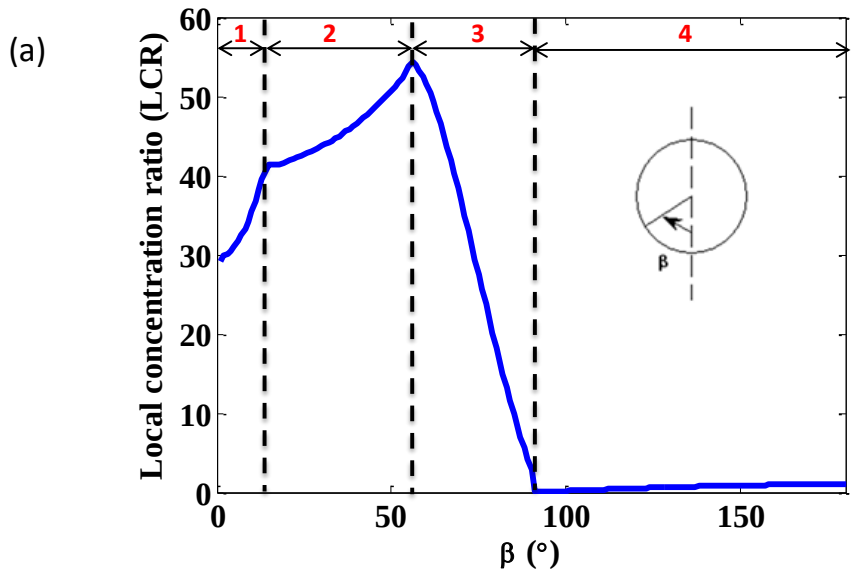

Fig. 3.3 Parabolic trough receiver (a) Local concentration ratio (LCR) around the receiver of a parabolic trough having rim angle 70° (data points taken from Ref. Jeter, 1986)

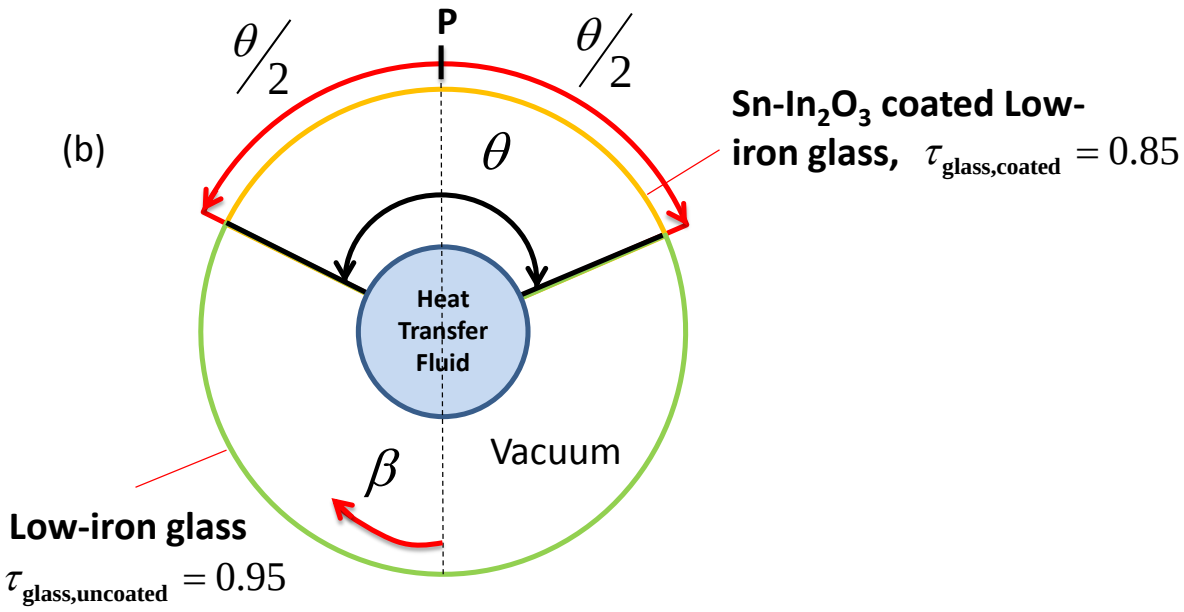

Fig. 3.3 Parabolic trough receiver (b) Schematic showing the regions of the hybrid glass envelope having different optical properties; θ denotes the angle up to which the glass envelope has been coated.

As discussed earlier, the amount of incident solar energy changes as we change the angle of the coating on the glass envelope. The transmissivity of the coated portion of the glass tube is taken to be 85 % whereas the transmissivity of the simple glass envelope without coating is taken to be 95 %. Hence as we increase the angle of the coating, the amount of transmitted solar energy decreases which leads to decrease in the optical efficiency. Figure 3.4 shows optical efficiency as a function of heat mirror circumferential angle.

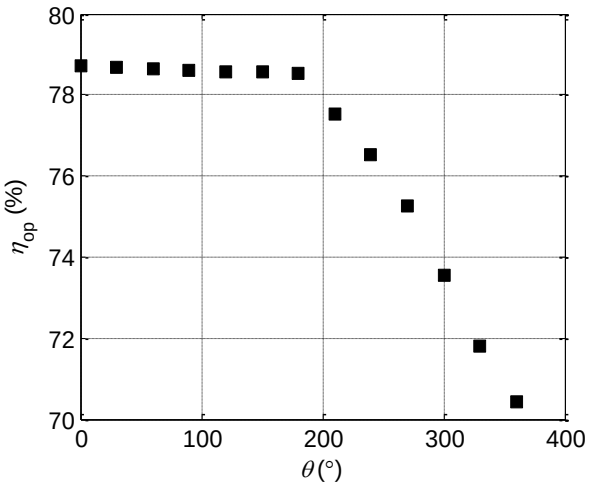

Fig. 3.4 Optical efficiency of parabolic trough as a function of heat mirror circumferential angle.

The present study is done for the rim angle (ψ) of 70°. For the rim angle of 70°, the concentration of the solar irradiation occurs up to the 180° of the receiver tube facing towards the parabolic trough (Jeter, 1986). It is clearly apparent from Fig. 3.4 that there is a critical heat mirror circumferential angle (θ = 180° in the present study) above which the optical efficiency sharply decreases. This is because coating is going into the region of the concentrated portion of the receiver tube. Hence θ should be carefully chosen to realize benefits of heat mirror in improving collector efficiency. θ should not overlap with the concentrated portion of the receiver tube. A large value of θ may help in reducing the thermal loss area, but at the same time large θ means sacrificing some optical efficiency (for instance in case θ >180°). Solar irradiation incident on the receiver tube $\bar{z}$ can be calculated by the following formula.

For $\theta \leq 180$

$$z = \rho\left[\left(\frac{\theta}{360}\right)\tau_h S + \left(\frac{30}{360}\right)\tau_g g_1 + \left(\frac{70}{360}\right)\tau_g g_2 + \left(\frac{80}{360}\right)\tau_g g_3 + \left(\frac{(180-\theta)}{360}\right)\tau_g S\right] \quad (3.4)$$

For $180 < \theta \leq 260$

$$z = \rho\left[\left(\frac{180}{360}\right)\tau_h S + \left(\frac{30}{360}\right)\tau_g g_1 + \left(\frac{70}{360}\right)\tau_g g_2 + \left(\frac{(\theta-180)}{360}\right)\tau_h g_3 + \left(\frac{(260-\theta)}{360}\right)\tau_g g_3\right] \quad (3.5)$$

For $260 < \theta \leq 330$

$$z = \rho\left[\left(\frac{180}{360}\right)\tau_h S + \left(\frac{30}{360}\right)\tau_g g_1 + \left(\frac{80}{360}\right)\tau_h g_3 + \left(\frac{(\theta-260)}{360}\right)\tau_h g_2 + \left(\frac{(330-\theta)}{360}\right)\tau_g g_2\right] \quad (3.6)$$

For $330 < \theta \leq 360$

$$z = \rho\left[\left(\frac{180}{360}\right)\tau_h S + \left(\frac{70}{360}\right)\tau_h g_2 + \left(\frac{80}{360}\right)\tau_h g_3 + \left(\frac{(\theta-330)}{360}\right)\tau_h g_1 + \left(\frac{(360-\theta)}{360}\right)\tau_g g_1\right] \quad (3.7)$$

$$\bar{z} = z.\alpha_m \quad (3.8)$$

where, g_1 is the average concentrated heat flux for 1st region ($330^o < \theta < 360^o$) (Fig. 3.3(a)), g_2 is the average concentrated heat flux for 2nd region ($260^o < \theta < 330^o$) (Fig. 3.3(a)), g_3 is the average concentrated heat flux for 3rd region ($180^o < \theta < 260^o$) (See Fig. 3.3(a)), ρ is the reflectivity of the aperture trough, S is the solar irradiation, z is the concentrated solar irradiations, $\bar{z}$ is the effective concentrated heat flux on the receiver tube, α_m is the absorptivity

of selectively coated metal receiver tube, θ is the angle of coating on the glass envelope, τ_h is the transmissivity of the coated portion of the glass envelope and τ_g is the transmissivity of the glass envelope, which is uncoated.

Overall energy balance

Once the amount of solar irradiance flux that is able to reach the selectively coated metal tube is known, the next step is to compute the overall energy balance. Energy balance equations were invoked for each component of the receiver. Firstly, the heat transfer from the absorber tube to the inner surface of the glass envelope has been analyzed. In this, mainly two kind of heat transfer mechanism takes place, one is by radiation and the second one is by convection. Since the system, which is considered here has vacuum in the annulus, so the heat transfer via convection mechanism will be negligible as compared to the radiation heat transfer. The convection heat transfer through the annulus could be modelled by an equivalent conduction heat transfer mechanism. Quantitatively, this could be realized through consideration of an equivalent conduction heat transfer coefficient to calculate the convection heat transfer. For vacuum configuration, the convection heat transfer become negligible, and the predominant mode of heat transfer is radiative heat transfer (See Eq. (3.9)). Next, the heat reaching the inner surface of the glass envelope is conducted to its outer surface (See Eq. (3.10)). Finally, the outer surface of the glass envelope rejects heat to the atmosphere through convective and radiative heat transfer mechanisms (See Eq. (3.11)).

$$Q_{\text{loss1}} = \frac{2\pi k_{\text{eff}} L(T_r - T_{ci})}{\ln\left(D_3 / D_2\right)} + \frac{\pi D_2 L\sigma(T_r^4 - T_{ci}^4)}{\frac{1}{\varepsilon_r} + \frac{1-\varepsilon_g}{\varepsilon_g}\left(\frac{D_2}{D_3}\right)} \tag{3.9}$$

$$Q_{\text{loss2}} = \frac{2\pi k_c L(T_{ci} - T_{co})}{\ln(D_4 / D_3)} \tag{3.10}$$

$$Q_{\text{loss3}} = \pi D_4 L h_f (T_{co} - T_a) + \varepsilon_g \pi D_4 L\sigma(T_{co}^4 - T_{\text{sky}}^4) \tag{3.11}$$

Under steady state conditions Eq. (3.12) below applies

$$Q_{\text{loss1}} = Q_{\text{loss2}} = Q_{\text{loss3}} = Q_{\text{loss}} \tag{3.12}$$

Calculation of the heat transfer coefficient

Firstly, the heat transfer occurring in between the HTF and receiver tube inner surface is calculated. This heat transfer occurs due to the convection mechanism so the convective heat transfer coefficient is calculated by the following equations. First of all the Reynold number (Re_f) of the flow is calculated. It will dictate whether the flow is laminar or turbulent.

$$Re_f = \frac{m_f D_1}{\mu_f A_1} \tag{3.13}$$

where, A_1 is the inner cross-section area of the receiver tube, D_1 is the inner diameter of receiver tube, v_f is the mass flow rate of the HTF in ms^{-1} and μ_f is the kinematic viscosity of heat transfer fluid, m_f is the mass flow rate of the HTF in kgs^{-1} which can be calculated from the following formula.

$$m_f = \rho_f v_f A_1 \tag{3.14}$$

If the Reynold number is less than 2300, then the flow has the laminar nature, and for laminar flow Nusselt number (Nu_f) is taken to be constant '4.36' (Incropera, F. P. and Dawitt, D. P., 2011).

If $Re_f < 2300$

Then $Nu_f = 4.36$

If the Reynold number is greater than 2300 then flow will be either in transition or of the turbulent nature, and for such flow the Nusselt number is calculated by the following formulae. (Duffie and Beckmen, 1993).

$$Nu_f = \frac{f_2/8 \left(Re_f - 1000\right) Pr_1}{1 + 12.7\sqrt{f_2/8}\left(Pr_1^{2/3} - 1\right)} \left(\frac{Pr_1}{Pr_2}\right)^{0.11} \tag{3.15}$$

$$f_2 = \left(1.82 log_{10}\left(Re_f\right) - 1.64\right)^{-2} \tag{3.16}$$

where, f_2 is the absorber tube's friction factor for inner surface, Pr_1 is the Prandtl number for HTF evaluated at T_f Temperature and Pr_2 is the Prandtl number evaluated at T_r Temperature.

Once the Nu_f is calculated, the convection coefficient (h_f) for the heat transfer is easy to calculate by the following formula

$$h_f = Nu_f \frac{k_f}{D_1} \tag{3.17}$$

where, k_f is the thermal conductivity of heat transfer fluid.

Now heat transfer from the glass envelope to the surroundings occurs through the convection and the radiation heat transfer mechanisms. For the convection heat transfer, it is required to calculate the convection heat transfer coefficient (h_a). For this, it is required to calculate the Reynold number (Re_a) of the flow by the following formula

$$Re_a = \frac{\rho_a v D_4}{\mu_a} \tag{3.18}$$

where, D_4 is the outer diameter of envelope tube, v is the wind speed across the glass envelope, μ_a is the kinematic viscosity of air and ρ_a is the density of air.

To calculate the Nusselt number it is required to know the constant which depends upon the Reynold number as in the Table [3.2].

$$Nu_a = C\, Re_a^m\, Pr_a^n \left(\frac{Pr_a}{Pr_4}\right)^{1/4} \tag{3.19}$$

where, C, m, n are constants, Pr is the average Prandtl number evaluated for T_a and T_4 temperatures, Pr_1 is the Prandtl number for HTF evaluated at T_f temperature, Pr_2 is the Prandtl number evaluated at T_r temperature and Pr_a is the Prandtl number of air evaluated at T_a temperature.

$$Pr = \frac{Pr_a + Pr_4}{2} \tag{3.20}$$

n = 0.37, if $Pr \leq 10$

n = 0.36, if $Pr > 10$

Table 3.2 constants values used for different range of Reynold number (Forristall, 2003)

Re_a	C	m
1-40	0.75	0.4
40-1000	0.51	0.5
1000-200000	0.26	0.6
200000-1000000	0.076	0.7

Once the Nusselt number has been calculated, the convection heat transfer coefficient (h_a) can easily calculated by the following formula.

$$h_a = Nu_a \frac{k_a}{D_4} \tag{3.21}$$

where, k_a is the thermal conductivity of air.

Calculation of the heat loss coefficient

Equivalent radiation heat transfer coefficient (h_r) can be calculated if the radiation heat losses are taken happening directly from the absorber tube instead of the glass envelope. After this it is easy to calculate the overall heat loss coefficient (see Eq. 3.29).

If A_{s2} is the outer surface area of the receiver tube, D_2 is the outer diameter of receiver tube and L is the length of the receiver tube or aperture, then thermal loss (Q_{loss}) can be calculated by the equations 3.22-3.29.

$$A_{s2} = \pi D_2 L \tag{3.22}$$

$$Q_{loss} = h_f A_{s2}(T_r - T_a) + \varepsilon_r \sigma A_{s2}(T_r^4 - T_{sky}^4) \tag{3.23}$$

$$\frac{Q_{loss}}{A_{s2}} = h_f (T_r - T_a) + \varepsilon_r \sigma (T_r^4 - T_{sky}^4) \tag{3.24}$$

$$\frac{Q_{\text{loss}}}{A_{s2}} = h_f (T_r - T_a) + \varepsilon_r \sigma (T_r^2 + T_{\text{sky}}^2)(T_r + T_a)(T_r - T_{\text{sky}}) \quad (3.25)$$

$$\frac{Q_{\text{loss}}}{A_{s2}} = (h_f + h_r)(T_r - T_a) \quad (3.26)$$

$$h_r = \frac{\varepsilon_r \sigma (T_r^4 - T_{\text{sky}}^4)}{(T_r - T_{\text{sky}})} \quad (3.27)$$

$$h_r (T_r - T_{\text{sky}}) = \varepsilon_r \sigma (T_r^2 + T_{\text{sky}}^2)(T_r + T_a)(T_r - T_{\text{sky}}) \quad (3.28)$$

$$U_L = \frac{Q_{\text{loss}}}{A_{s2}(T_r - T_a)} \quad (3.29)$$

Calculation of various factors

Collector efficiency factor (F') basically represent the ratio of useful gain in energy to the useful energy gain which would be absorbed by the collector absorbing surface. F' is a constant for a given system design and the fluid flow rate.

Collector heat removal factor (F_r) relates the actual useful gain in energy to the energy gain by the fluid if the whole receiver were at HTF inlet temperature. To represent F_r a new factor, collector flow factor F'' can be defined. (See Eqs. 3.30-3.32)

$$F' = \frac{1/U_L}{\frac{1}{U_L} + \frac{D_2}{h_f D_1} + \left(\frac{D_2}{2k_r} \ln\left(\frac{D_2}{D_1}\right)\right)} \quad (3.30)$$

$$F'' = \frac{m_f Cp_f}{A_{s2} U_L F'} \left[1 - \exp\left(-\frac{A_{s2} U_L F'}{m_f Cp_f}\right)\right] \quad (3.31)$$

$$F_r = F' \times F'' \quad (3.32)$$

where, A_{s2} is the outer surface area of the receiver tube, Cp_f is the specific heat of heat transfer fluid, D_1 is the inner diameter of receiver tube, D_2 is the outer diameter of receiver tube, F' is the collector efficiency factor, F'' is the collector flow factor, F_r is the collector

heat removal factor, h_f is the convective heat transfer coefficient for fluid flowing in the receiver tube, k_r is the thermal conductivity of metal receiver tube, m_f is the mass flow rate of the HTF, and U_L is the overall loss coefficient.

3.4 Algorithm

A code has been written in MATLAB to solve the aforementioned governing energy balance equations. Subsequent paragraphs describe the algorithm which has been essentially implemented to calculate the performance parameters (such as thermal losses or thermal efficiency of the system) through solution of energy balance equations.

For a known steady state absorber tube temperature (T_r), the resulting temperatures of the glass envelope $(T_{co} \text{ and } T_{ci})$ and the heat loss (Q_{loss}) have been found by solving the aforementioned equations (Eqs. (3.9) - (3.12)) using an iterative process.

Firstly, Eq. (3.11) was solved for Q_{loss3} by assuming some outer glass envelope temperature (T_{co}). The calculated loss occurring from envelop to atmosphere (Q_{loss3}) was then equated in Eq. (3.10) to find inner glass envelope temperature (T_{ci}). Next, the calculated inner glass envelope temperature was used in Eq. (3.9) to find the resulting heat loss term (Q_{loss1}). Finally, the calculated loss terms Q_{loss1} and Q_{loss3} were compared. If the difference was negligible then the assumed/calculated temperatures (T_{ci}, T_{co}) and the resulting loss term were in well agreement and the corresponding energy balance equations were satisfied. In case a significant difference between calculated loss terms Q_{loss1} and Q_{loss3} was observed then the whole process was carried out for a new value inner glass envelop temperature (T_{ci}). The iterative process was carried until the difference between calculated loss terms Q_{loss1} and Q_{loss3} became insignificant.

Now with the help of the calculated heat loss term the overall heat loss coefficient U_L was evaluated (see Eq. (3.29)).

Next, the collector efficiency factor F' was calculated (see Eq. (3.30)). With the help of collector efficiency factor, collector flow factor F'' and the collector heat removal factor F_r

were evaluated (see Eqs. (3.31) and (3.32)). F_r Reflects the thermal energy gain by the working fluid as in transverses through the receiver length.

Now since we know the overall heat loss coefficient and the collector heat removal factor, it can easily find the loss in the concentrating heat flux using Eq. (3.33).

$$z_{\text{loss}} = F_r A_{s_2} U_L \left(T_r - T_a\right) \tag{3.33}$$

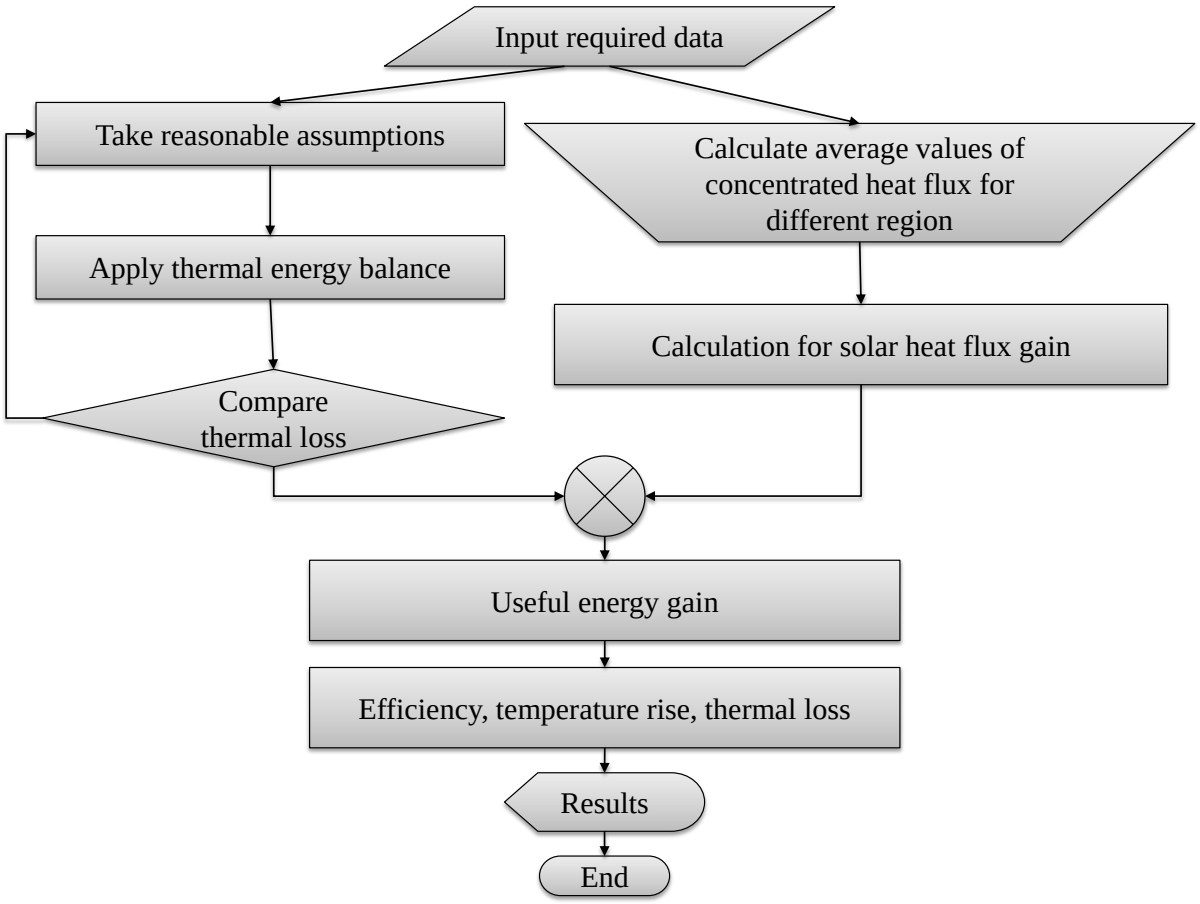

Fig. 3.5 Algorithm to implement the formulation for solution in MATLAB

Now since the concentrating heat flux loss is known, the useful heat gain can easily be evaluated by using Eq. (3.33). And once the useful heat gain is known, the temperature rise of HTF, the thermal efficiency of the system, the optical efficiency of the system can be easily calculated using Eq. (3.34-3.38).

$$Q_{\text{usefull}} = \left(F_r A_{s2} \bar{z} - z_{\text{loss}}\right) \tag{3.34}$$

$$Q_{\text{usefull}} = \left(F_r A_{s2} \bar{z} - F_r A_{s_2} U_L \left(T_r - T_a\right)\right) \tag{3.35}$$

$$\Delta T = \frac{Q_{\text{usefull}}}{m_f Cp_f} \tag{3.36}$$

$$A_{ap} = L\left(W - D_2\right) \tag{3.37}$$

$$\eta_{\text{thermal}} = \frac{Q_{\text{usefull}}}{(SA_{ap})} \tag{3.38}$$

$$\eta_{\text{optical}} = \frac{\bar{z}A_{s_2}}{(SA_{ap})} \tag{3.39}$$

Chapter 4

Results and Discussion

4.1 Introduction

As discussed in the previous chapters, a code has been written in MATLAB (R2010b) to implement the formulation. A novel receiver tube design has been proposed. Solution of the optical and the overall energy balance equations fetch us evaluation of performance parameters such as optical and thermal losses (convection and radiation losses), useful heat gain, and thermal efficiency, optical efficiency, and the rise in temperature of the HTF. In order to truly capture the performance of such novel collectors (employing hybrid glass envelope) it is imperative to study the effect of design (such as heat mirror circumferential angle) and operating parameters (such as absorber temperature, HTF flow rate and wind speed), on the aforesaid performance parameters. It was found that mainly three factors that is absorber tube temperature, wind speed and heat mirror angle are instrumental in deciding the overall efficiency of the system.

4.2 Effect of absorber tube temperature

Firstly, for different values of heat mirror circumferential angles (θ) glass envelope temperature has been evaluated as a function of selectively coated absorber tube temperature (see Fig. 4.1 (a)). It is apparent from the plots that envelope temperature increases nonlinearly with increase in absorber temperature. This can be understood from the fact that heat transfer mechanism from the absorber tube to the glass envelope is predominantly radiation, therefore with linear increase in absorber tube temperature, the heat transfer from the absorber tube to the glass envelope varies as T_r^4.

Now, as the convection and radiation losses finally take place from the glass envelope to the surrounding/sky therefore these also increase nonlinearly with absorber tube temperature (see Fig. 4.1 (b); 4.1 (c) and 4.1 (d)). As for as the effect of circumferential heat mirror angle is concerned, it can be seen that with increase in θ, the envelope temperature and hence the thermal losses decrease.

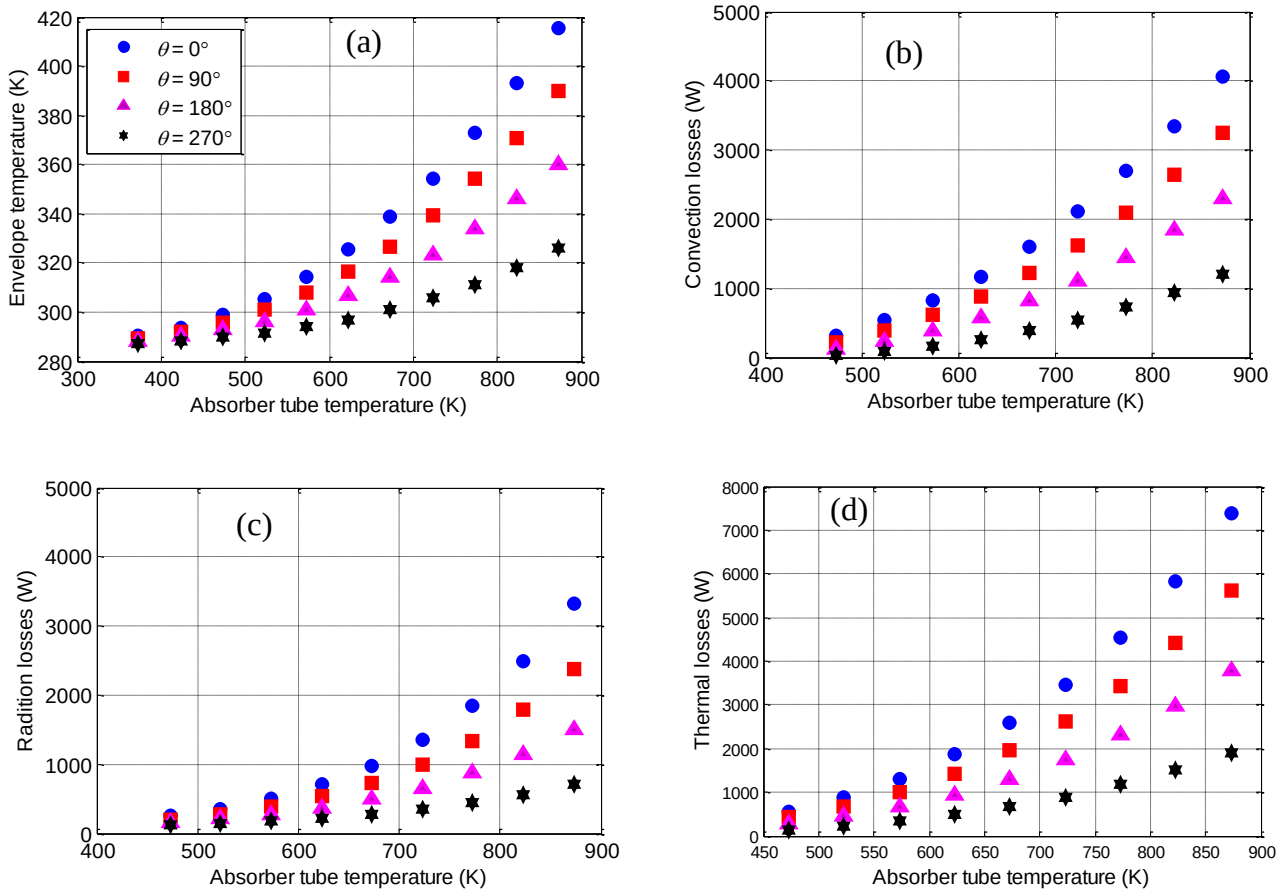

Fig. 4.1 For different values of circumferential heat mirror angles,4.1 (a) envelope temperature as function absorber tube temperature,4.1 (b) convection losses as function absorber tube temperature,4.1 (c) radiation losses as function absorber tube temperature, and 4.1 (d) total thermal losses as function absorber tube temperature.

However, the thermal efficiency does not follow the same trend (See Fig. 4.2) i.e. thermal efficiency is not always highest for the case of maximum circumferential angle (θ = 270°), instead thermal efficiency is initially highest for (θ = 180°) and as the absorber temperature increase the efficiency for (θ = 270°) takes over. This could be understood from the fact that for relatively lower absorber tube temperatures the thermal losses are relatively low, therefore it is beneficial to coat the glass envelope up to θ = 180°, as higher θ values shall entail higher optical losses. On the other hand as the absorber tube temperature rises to a very high value the thermal losses escalate and it is imperative to increase θ to 270° to reduce the ever-increasing thermal losses.

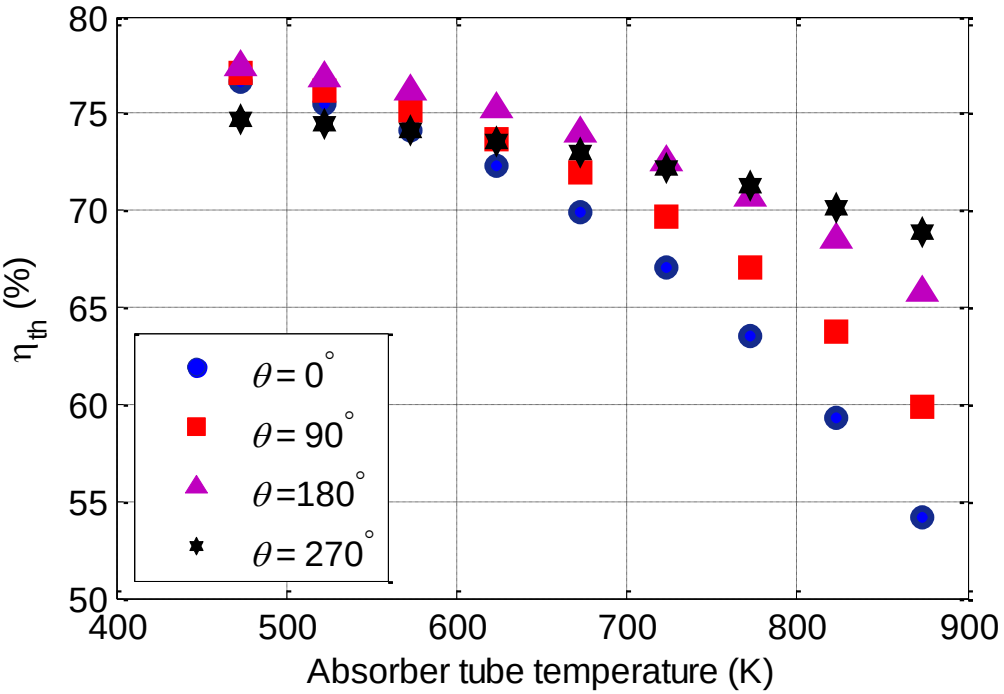

Fig. 4.2 Thermal efficiency as a function of absorber tube temperature for different circumferential heat mirror angles.

4.3 Effect of wind speed

Next, the effect of wind speed is considered for various values of heat mirror angles. It can be seen from Fig. 4.3 (a) that radiative losses decrease with increase in wind speed. This could be understood from the fact that under steady state conditions, high wind speed means lesser outer glass cover temperature and hence lesser radiative losses. As for as convection heat losses are concerned they follow the expected trend i.e. they increase with wind speed (See Fig. 4.3 (b)) owing to increase in the value of the convective heat transfer coefficient. Overall the thermal losses do not vary much with wind speed owing to the aforementioned opposing convection and radiation losses trends.

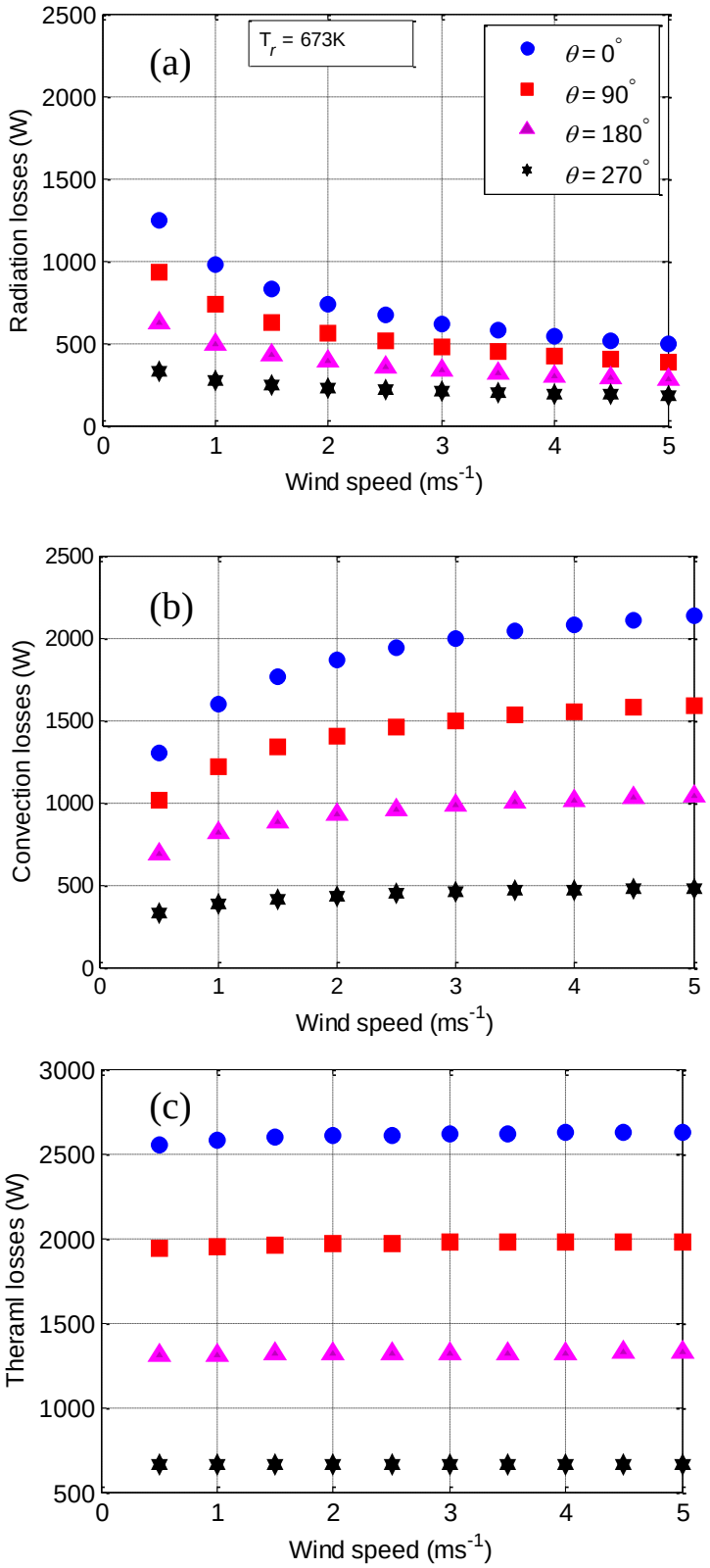

Fig. 4.3 For a given absorber tube temperature and for different values of θ, 4.3 (a) radiation losses as a function of wind speed, 4.3 (b) convection losses as a function of wind speed, and 4.3 (c) thermal losses as a function of wind speed.

4.4 Effect of heat mirror angle

Finally, the circumferential heat mirror angle is varied and its effect on the performance of the system is analysed for different absorber tube temperatures. Figure 4.4 (a) and 4.4 (b) clearly show that for a given θ, losses are highest for the highest absorber tube temperature. Furthermore, the effect of absorber tube temperature diminishes as θ is increased from 0° to 270° (temperature isotherms tend to converge with increase in θ). This can be understood from the fact that at high θ values essentially thermal energy radiated by the absorber tube to the inner cover of the glass envelope is reflected back to the absorber tube; hence the increased absorber tube temperature does not correspondingly result in increased thermal losses.

Figure 4.4 (c) deciphers a very interesting characteristic of such novel solar thermal systems. Clearly, thermal efficiency increase with increase in θ only up to a certain value of θ., a value higher than this critical value tends to decrease the thermal efficiency. Although, thermal losses are always decreasing with increase in θ, but due to anomalous nature (See Fig. 3.4) of optical efficiency, the efficiency does not always increase with increase in θ, instead it dips down in accordance with the optical efficiency of the system.

When θ is increased from a value 0° to a value $\leq$ 180°, the decrease in thermal losses area dominates over the increase in the optical losses but as we increase θ beyond 180°, drastic increase in optical losses occur which dominates over the decrease in thermal loss area and hence the thermal efficiency of the system tends to decrease. Therefore, the system has the highest efficiency at 180 ° circumferential heat mirror angle.

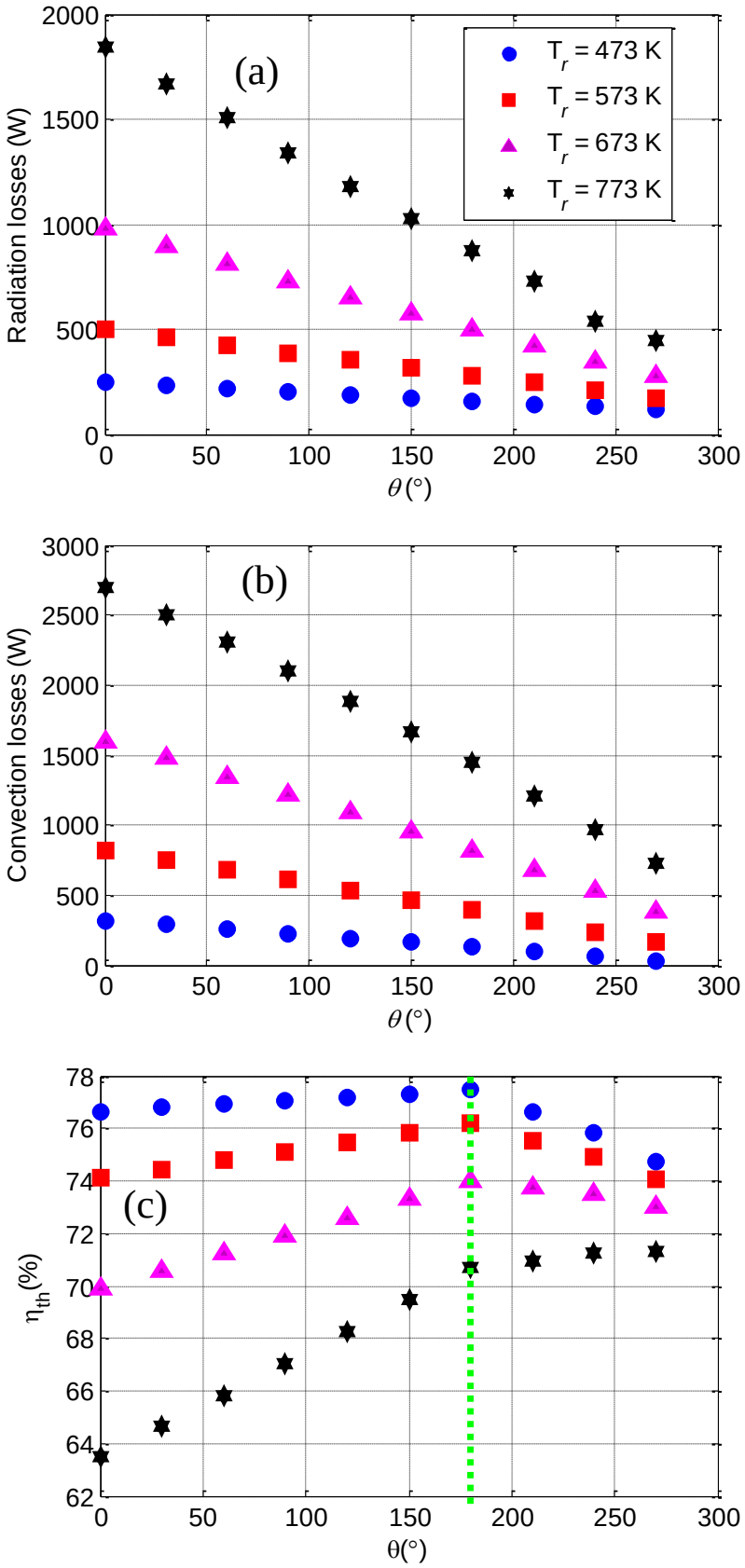

Fig. 4.4 For various absorber tube temperatures, 4.4 (a) radiation losses as a function of θ, 4.4 (b) convection losses as a function of θ, and 4.4 (c) thermal efficiency as a function of θ.

Chapter 5

Conclusion and Future Scope

5.1 Conclusions

The present study highlights the fact that through usage of hybrid glass envelope (having coated and uncoated portions) it is possible to engineer a parabolic receiver design that has 3-12% higher thermal efficiency as compared to its surface absorption based counterpart. The uncoated portion ensures high transmittance in the solar irradiance wavelength band and the coated portion ensures high reflectivity in the mid-infrared region. The aforementioned characteristics lend it to reduce thermal loss area without compromising with the optical efficiency of the system.

Following paragraphs briefly describe the key conclusions from the present work

- With the linear increase in absorber tube temperature, glass envelope temperature does not change linearly because of the predominating effect of the radiation heat transfer in the annulus. Convection and radiation heat losses are directly dependent upon the glass envelope temperature, therefore the effect of respective heat losses are also nonlinear. As for the effect of the heat mirror angle is concerned, the envelope temperature and thermal losses decrease with increase in heat mirror angle.
- As for the effect of wind speed is concerned, radiation losses decrease with increase in wind speed but the convection losses increases with the increase in wind speed. High wind speed means lesser glass temperature, resulting in to less radiation loss. Whereas convection loss increases due to turbulence around the receiver tube. But the thermal losses is not effected much doe to contrast nature of convection and radiation losses.
- With the increase in heat mirror angle, the radiation heat loss and convection heat loss both decrease. Initially, optical losses remain constant with increase in heat mirror angle, however, after a certain critical heat mirror angle, they tend to drastically increase with increase in heat mirror angle. Due to the two aforesaid opposing tendencies (variation of optical and thermal loss with heat mirror angle), the overall efficiency of the system first increases up to certain point and then starts decreasing owing to predominance of high optical losses.

Therefore, for a given rim angle of the parabolic trough, there exists a critical value of circumferential heat mirror angle (θ) which denotes the maximum angle up to which the envelope should be coated with Sn-In_2O_3. Heat mirror angles exceeding this critical value instead decrease the optical and hence thermal efficiency of the system.

5.2 Future scope

1. Now that it has been theoretically proved that the proposed novel design has higher thermal efficiencies as compared to the conventional design (for optimum values of heat mirror angles). The present work could be extended for experimental validation in order to truly assess the potential of such novel receiver designs. Therefore, experimental investigation into such receiver designs is warranted.
2. In the present work, the analysis has been restricted for a particular rim angle. This is another parameter which could be investigated in greater detail i.e., the effect of rim angle, on the value of optimum heat mirror angle could be evaluated.

References

Ansary H. A. and Zeitoun, O. (2011). Numerical study of conduction and convection heat losses from a half-insulated air-filled annulus of the receiver of a parabolic trough collector, *Solar Energy, 85*, 3036-3045.

Arasu, V. and Sornakumar, T. (2006). Performance characteristics of parabolic trough solar collector system for hot water generation. *International Energy journal, 07*(2), 137-145.

Bergman, T. L., Lavine, A. S., Incropera, F. P. and Dewitt, D. P. (2011). Fundamentals of heat and mass transfer. 7th edition, John Wiley and Sons Inc., Hoboken, New Jersey.

Cheng, Z. D., He, Y. L., Cui, F.Q., Xu, R. J. and Tao, Y. B. (2012). Numerical simulation of a parabolic trough solar collector with non-uniform solar flux conditions by coupling FVM and MCRT method. *Solar Energy, 86*, 1770-1784.

Cheng, Z. D., He, Y. L., Wang, K., Du, B. C. and Cui, F. Q. (2014). A detailed parametric study on the comprehensive characteristics and performance of a parabolic trough solar collector system. *Applied Thermal Energy, 63*, 278-289.

Dudley, V. E., Msi, G., Evans, L. R., and Matthews, C. W. (1995). Test Results, Industrial Solar Technology Parabolic Trough Solar Collector. *Sandia National Labs.*, Albuquerque, NM (USA).

Duffie, J. A., and Beckman, W. A. (1993). Solar engineering of thermal processes, 4th edition, John Wiley and Sons Inc., Hoboken, New Jersey.

Egbo, G., Sintani, I. S. and Dandkouta, H. (2014). Simulation of annular gap effect on performance of solar parabolic-trough collector model TE38 in Bauchi. *American Journal of Engineering Research, 03*(12), 102-108.

Fan, J. C., and Bachner, F. J. (1976). Transparent heat mirrors for solar-energy applications. *Applied Optics, 15*(4), 1012–1019.

Fan, J. C., Bachner, F. J., Foley, G. H. and Zavracky. P. M. (1974). Transparent heat mirror films of TiO2 / Ag / TiO2 for solar energy collection and radiation insulation. *Applied Physics Letters, 25*(12), 693–695.

Forristall, R. (2003). *Heat transfer analysis and modelling of a parabolic trough solar receiver implemented in Engineering Equation Solver*. National Renewable Energy Technology, TP 550-34169.

Galindo, J. and Bilgen, E. (1984). Flux and temperature distribution in the receiver of parabolic solar furnaces. *Solar Energy, 33*, 125-135.

He, Y. L., Xiao, J., Cheng Z. D. and Tao, Y. B. (2011). A MCRT and FVM coupled simulation method for energy conversion process in parabolic trough solar collector, *Renewable Energy, 36,* 976-985.

Jeter, S. M. (1986). Calculation of the concentrated flux density distribution in parabolic trough collectors by a semifinite formulation. *Solar Energy, 37*(5), 335-345.

Jeter, S. M. (1987). Analytical determination of the optical performance of practical parabolic trough collectors from design data. *Solar Energy 39*(1), 11-21.

Khanna, S., Singh, S. and Kedare, S. B. (2014). Effect of angle of incidence of sun rays on the bending of absorber tube of solar parabolic trough collector. *Energy Procedia, 48,* 123-129.

Khullar, V. (2015). Heat transfer analysis and optical characterization of nanoparticle dispersion based solar thermal systems, PhD Thesis, Indian institute of technology, Ropar.

Liang, H., You, S. and Zhang, H. (2015). Comparison of different heat transfer models for parabolic trough solar collectors. *Applied Energy, 148,* 105-114.

Manikandan, K. S., Kumaresan, G., Velraj R. and Iniyan, S. (2012). Parametric study of solar parabolic trough collector system. *Asian Journal of Applied Science, 10,* 1-10.

Marif, Y., Benmoussa, H., Nouguettaia, H., Belhadj, M. M. and Zerrouki, M. (2014). Numerical simulation of solar parabolic trough collector performance. *Energy Conversion and Management, 85*, 521-529.

Mohamed, E. A. (2013). Design and testing of a solar parabolic concentrating collector. *Renewable Energy and Power Quality Journal, 11*, 1-7.

Padilla, R. V., Demirkaya, G., Goswami, D. Y. and Stefanakos, E., (2011). Heat transfer analysis of parabolic trough solar collector. *Applied Energy, 88*, 5097-5110.

Paetzold, J., Cochard, S., Vassallo A. and Fletcher, D. F. (2014). Wind engineering analysis of parabolic trough solar collectors: The effect of varying the trough depth. *Journal of Wind Engineering and Industrial Aerodynamics, 135*, 118-128.

Taylor, R. A., Hewakuruppu, Y., Dejarnette, D. and Otanicar, T. P. (2015). Fabrication and comparison of selective, transparent optics for concentrating solar systems. *SPIE 9559*.

Taylor, R. A., Hewakuruppu, Y., Dejarnette, D. and Otanicar, T. P. (2016). Comparison of selective transmitters for solar thermal application. *Applied Optics, 55*(14), 3829-3839.

Thomas, A. and Guven, H. M. (1994). Effect of optical errors on flux distribution around the absorber tube of a parabolic trough concentrator. *Energy Conversion and Management, 35*(7) 575-852.

Tijani, S. and Roslan, A. M. S. B. (2014). Simulation analysis of thermal losses of parabolic trough solar collector in Malaysia using computational fluid dynamics. *Procedia Technology, 15,* 841-848.

Wang, Y., Liu, Q., Lei, J. and Jin, H. (2015). Performance analysis of a parabolic trough solar collector with non-uniform solar flux conditions. *International Journal of Heat and Mass Transfer, 82,* 236-249.

Xu, C., Chen, Z., Li, M., Zhang, P., Ji, X., Luo, X. and Liu, J. (2014). Research on the compensation of the end loss effect for parabolic trough solar collectors. *Applied Energy 115,* 128-139.

Yang, B., Zhao, J., Xu, T. and Zhu, Q. (2010). Calculation of the concentrated flux density distribution in parabolic trough solar concentrated by Monte Carlo Ray-Trace method. *IEEE,* 9784, 4244-4964.

Yilmaz, I. H. and Soylemez, M. S. (2014). Thermo-mathematical modelling of parabolic trough collector. *Energy Conversion and Management, 88,* 768-784.

Zemler, M. K., Bohl, G., Rios, O. and Boetcher, S. K. S. (2013). Numerical study of wind forces on parabolic solar collectors. *Renewable Energy, 60,* 496-505.

APPENDIX

APPENDIX A - *Geometric specifications*

Table 6.1 geometric properties of the PTC system (Dudley V. E. et al., 1994).

L (m)	fl (m)	W (m)	D_2 (m)	D_4 (m)	t_r (m)	t_g (m)	ψ (°)
7.8	1.4	5	0.07	0.115	0.003	0.003	70

APPENDIX B - *Optical properties of the PTC system*

Table 6.2 optical properties of the PTC system (Dudley V. E. et al., 1994)

	Absorptivity	Transmissivity	Emissivity	Reflectivity
Metal tube	0.96	-	0.14	-
Glass tube	0.05	0.95	0.88	-
Heat mirror coating	0.13	0.85	-	-
Trough	-	-	-	0.93

APPENDIX C – *Input parameters*

Table 6.3 Input parameters

Heat mirror angle (θ) (°)	Wind speed (v) (ms^{-1})	Absorber tube temperature (T_r) (K)	HTF mass flow rate (v_f) (lts^{-1})	Solar irradiation (S) (Wm^{-2})
0-360	0.5-5.0	373-873	18.4-56.8	807.9

List of publications

Mahendra, P., Khullar, V., Mittal, M., "Applicability of heat mirrors in reducing thermal losses in concentrating solar collectors", Paper No. IMECE2016-66565, *ASME International Mechanical Engineering Congress and Exposition*, Phoenix, Arizona, USA, Nov. 11-17, 2016.